Supplementary Material

^{18}F-Flurpiridaz PET Segmental and Territory Myocardial Blood Flow Metrics: Incremental Value Beyond Perfusion for CAD Categorization

René R. Sevag Packard[1,2,3], John R. Votaw[4], C. David Cooke[4,5], Kenneth F. Van Train[5], Ernest V. Garcia[4], Jamshid Maddahi[1,6]

[1] Division of Cardiology, Department of Medicine, David Geffen School of Medicine, University of California, Los Angeles, California

[2] Ronald Reagan UCLA Medical Center, Los Angeles, California

[3] Veterans Affairs West Los Angeles Medical Center, Los Angeles, California

[4] Department of Radiology and Imaging Sciences, Emory University School of Medicine, Atlanta, Georgia

[5] Syntermed, Inc., Atlanta, Georgia

[6] Nuclear Medicine Clinic, Department of Molecular and Medical Pharmacology, David Geffen School of Medicine, University of California, Los Angeles, California

Short Running Title:

Myocardial Blood Flow for CAD Categorization

SUPPLEMENTARY METHODS

Study Protocol

^{18}F-flurpiridaz doses were pre-specified as 2.5-3.0 mCi for rest and 6.0-6.5 mCi for pharmacologic stress (≥30 minutes between rest and pharmacological stress).[1] Consumption of caffeine-containing beverages, food, or medications within 12 hours prior to the test was prohibited. Pharmacological stress was conducted with regadenoson, adenosine, or dipyridamole, and ^{18}F-flurpiridaz was administered during the peak vasodilatory effect according to the package insert. The reference standard was quantitative invasive coronary angiography assessed in a blinded manner (PERFUSE Core Laboratories and Data Coordinating Center, Boston, MA). In the present study, significant CAD was defined as either ≥50% stenosis, ≥70% stenosis, or 50-69% stenosis (as indicated) in at least one coronary artery for receiver operating characteristic (ROC) area under the curve (AUC) analyses. Segmental rest myocardial blood flow (in $mL*min^{-1}*g^{-1}$), stress myocardial blood flow, myocardial flow reserve, and relative flow reserve values were stratified on a per-vessel basis according to increasing levels of CAD burden, i.e. normals, and 0-29%, 30-49%, 50-69%, and 70-100% stenoses.[2] ROC analyses were performed on a per-vessel basis, where the lowest flow metric in a given coronary territory was paired with the highest stenosis in the same coronary artery.[2] ROC analyses were also conducted on a per-patient basis, where the lowest flow metric in any coronary territory was paired with the highest stenosis in any coronary territory.[2] Normals were defined as having <30% stenosis, left ventricular ejection fraction (LVEF) ≥50%, and absence of hypertension, diabetes mellitus, previous myocardial infarction, coronary revascularization, or heart failure.

Quality Control

Pharmacological stress studies from the ^{18}F-flurpiridaz phase III trial underwent a 2-step quality control, both of which were blinded: an initial one from the trial core lab (BioClinica, Inc., Newtown, PA), followed by a second one from investigators of the present study. In the phase III trial, pharmacological stress studies were not required to have adequate time-activity curves for myocardial blood flow analyses. Of the n=557 pharmacological stress patients evaluated from the phase III trial, the following were excluded (**Fig. 1**): n=233 with missing or inadequate kinetic data, n=8 with no invasive coronary angiography data, n=31 with prior myocardial infarction, and n=40 with a poor fit of the calculated flow curves to the measured flow curves (defined as χ^2 >12). Thus, there were n=245 studies suitable for flow analyses.

For rest and stress MBF determination, no filtering or noise reduction was used on dynamic short axis data. All the kinetic data was motion corrected, using a minimization of the entropy of each frame compared to a reference frame. The reference frame was determined by a quality control procedure as follows. Alignments were performed between frames (n,n-1), (n,n-2), and (n-1,n-2) and checked for consistency. That is, the registration (n,n-1) $*$ (n-1,n-2) had to match the registration (n,n-2) to within the size of the pixel. Initially, n was the last frame. If this triple of frames did not pass the quality control, then n was set to the next to last frame and the process was repeated until a good triple of frames is found. The reference frame was then set to n.

Kinetic data was collected up to the frame closest to, but not greater, than 240 sec from ^{18}F-flurpiridaz injection. Automatic parameters (center, radius of search, apex, and base) were identified (Emory Cardiac Toolbox v4), quality controlled, and modified when necessary. Tissue regions of interest (ROI) were calculated on a summed image of 120-240 sec as the centerline from the maximal count sampling of the myocardium ± 3 mm. The blood input ROI was a 10 mm diameter sphere placed at the point of peak activity, outside the base (on a median filtered image) on the frame with peak left atrial activity. To verify adequate radiopharmaceutical delivery, data acquisition, and patient compliance, automated quality control algorithms assessed rest and stress time-activity curves for (i) inconsistent frame duration, (ii) scanner saturation, (iii) inability to detect the blood curve peak, (iv) inappropriate blood peak width, (v) flat blood curve tail, (vi) gradual patient motion, and (vii) abrupt patient motion.[3] When problems were detected in either the stress or rest data, a message was sent to the user indicating which curve was identified and what quality control parameter was out of range.

A 1-tissue compartment model was implemented as previously described,[4] using a one rate-constant (microsphere analog) model with spillover effects to describe radiopharmaceutical uptake in the myocardium. Count recovery coefficients to correct for finite scanner spatial resolution were fixed at 0.8 for tissue and 0.95 for blood; blood volume (the fraction of tissue occupied by blood) was set at 0.05. The spillover coefficients were free parameters during the fitting procedure. Spillover from tissue to blood was determined by fitting the global average tissue uptake with three parameters: global flow, spillover from blood to myocardium, and spillover from myocardium to blood.

No relation was assumed between the spillover coefficients. The corrected blood curve from this fit was used as the input function for all segmental flow determinations. The goodness-of-fit χ^2 measure was used for fitted curves, and studies with a χ^2 >12 were excluded from analyses due to poor fit.

All pixels in the heart were used to calculate the corrected blood curve from this fitting operation. It was then used to determine K1 in each of the 3 coronary territories and 17 segments. K1 and the 2 spillover variables (from the blood pool to the myocardium due to imperfect spatial resolution, and from the myocardium to the blood pool due to imperfect spatial resolution, ventricular contraction, and respiration) were determined by minimizing a figure of merit using Powell's algorithm. The figure of merit was the summation of the difference between the measured data and model estimate, weighted by frame duration. The myocardial extraction fraction correction of ^{18}F-flurpiridaz was set using a simplified equation: K1 = 0.94 $*$ flow, as previously described.[4]

SUPPLEMENTARY REFERENCES

1. Maddahi J, Lazewatsky J, Udelson JE, Berman DS, Beanlands RSB, Heller GV et al. Phase-III clinical trial of fluorine-18 flurpiridaz positron emission tomography for evaluation of coronary artery disease. *J Am Coll Cardiol* 2020;**76**:391-401.
2. Packard RRS, Cooke CD, Van Train KF, Garcia EV, Maddahi J. Diagnostic performance of automated myocardial blood flow quantitation by flurpiridaz F18 positron emission tomography: a sub-study of the flurpiridaz F18 clinical trial (abstr). *J Nucl Med* 2020;**61**,Suppl1:652.
3. Van Tosh A, Votaw JR, David Cooke C, Cao JJ, Palestro CJ, Nichols KJ. Relationship of (82)Rb PET territorial myocardial asynchrony to arterial stenosis. *J Nucl Cardiol* 2020;**27**:575-588.
4. Packard RRS, Huang SC, Dahlbom M, Czernin J, Maddahi J. Absolute quantitation of myocardial blood flow in human subjects with or without myocardial ischemia using dynamic flurpiridaz F18 PET. *J Nucl Med* 2014;**55**:1438-44.
5. Packard RRS, Cooke CD, Van Train KF, Votaw JR, Sayre JW, Lazewatsky JL et al. Development, diagnostic performance, and interobserver agreement of a (18)F-flurpiridaz PET automated perfusion quantitation system. *J Nucl Cardiol* 2020, Epub.

SUPPLEMENTARY FIGURES AND TABLE

Suppl. Figure 1A. Segmental Rest Myocardial Blood Flow and CAD Severity in Pooled Coronary Territories.

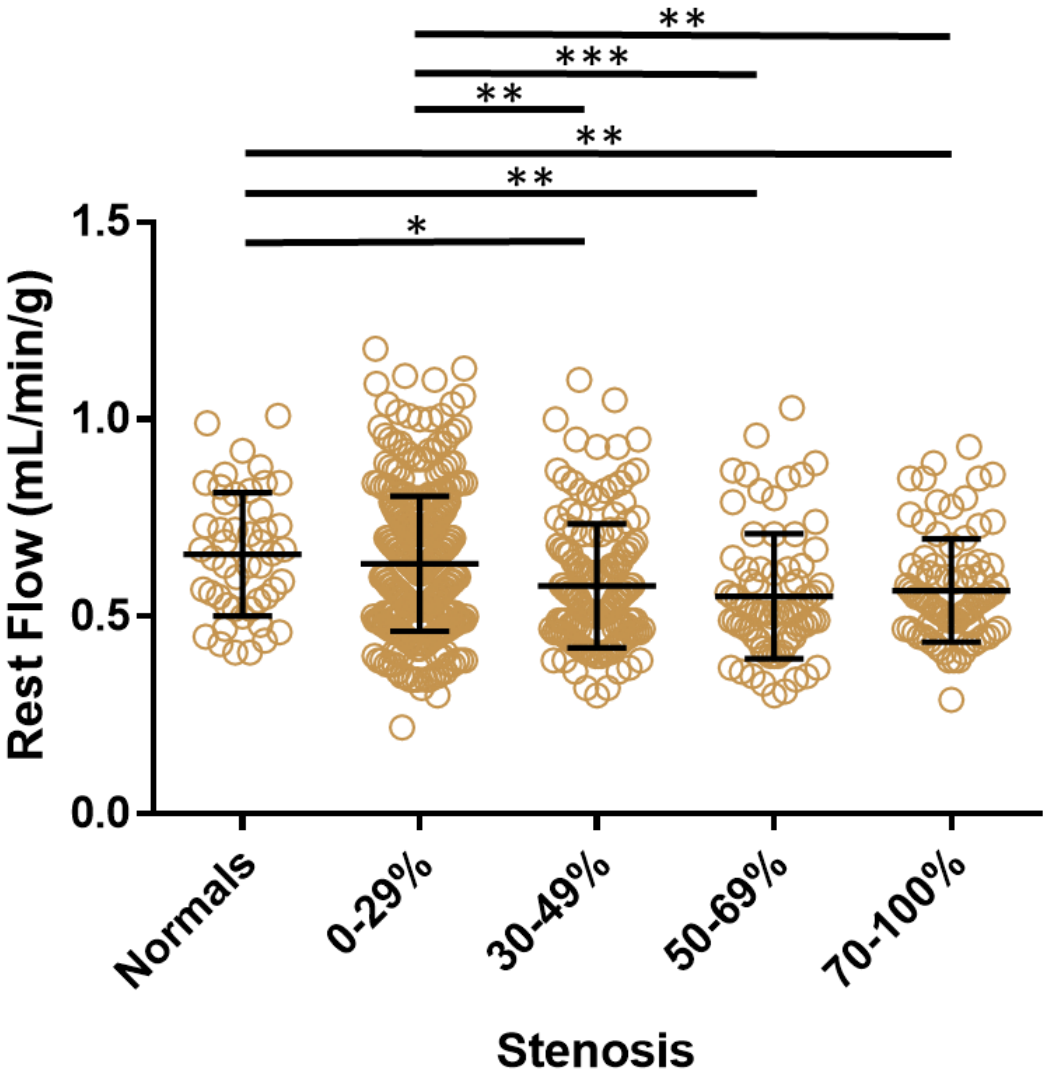

Segmental rest flow had limited discriminatory ability to detect increasing stenoses in pooled coronary territories, decreasing from 0.66±0.16 $mL*min^{-1}*g^{-1}$ in normals (n=48), to 0.63±0.17 in 0-29% stenosis (n=371), 0.58±0.16 in 30-49% stenosis (n=153), 0.55±0.16 in 50-69% stenosis (n=77), and 0.57±0.13 in 70-100% stenosis (n=86) groups (*P<0.05, **P<0.01, ***P<0.001).

Suppl. Figure 1B. Segmental Rest Myocardial Blood Flow and CAD Severity in the LAD.

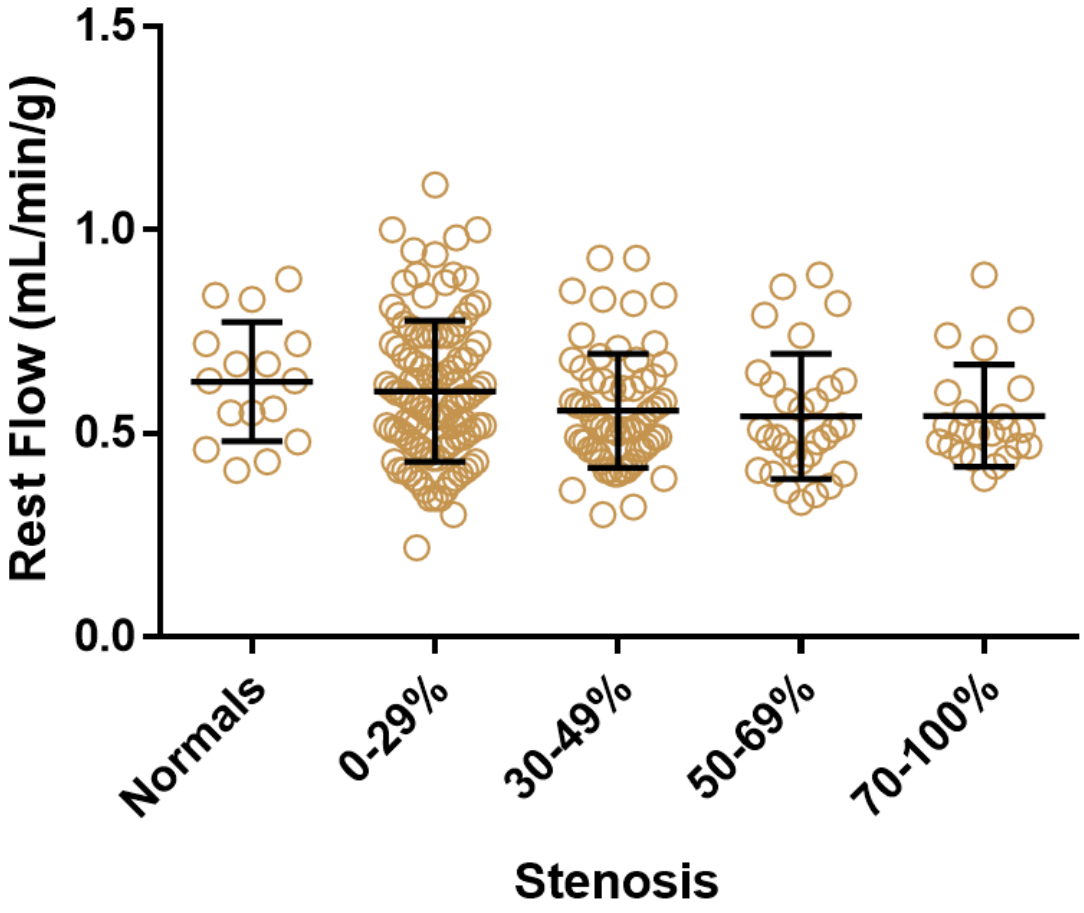

In the LAD territory, there was no significant correlation between segmental rest flow and stenosis burden. The segmental rest flow was 0.63 ± 0.15 $mL*min^{-1}*g^{-1}$ in normals (n=16), 0.60 ± 0.17 in the 0-29% stenosis (n=111), 0.56 ± 0.14 in the 30-49% stenosis (n=65), 0.54 ± 0.15 in the 50-69% stenosis (n=30), and 0.54 ± 0.13 in the 70-100% stenosis (n=23) groups.

Suppl. Figure 1C. Segmental Rest Myocardial Blood Flow and CAD Severity in the LCx.

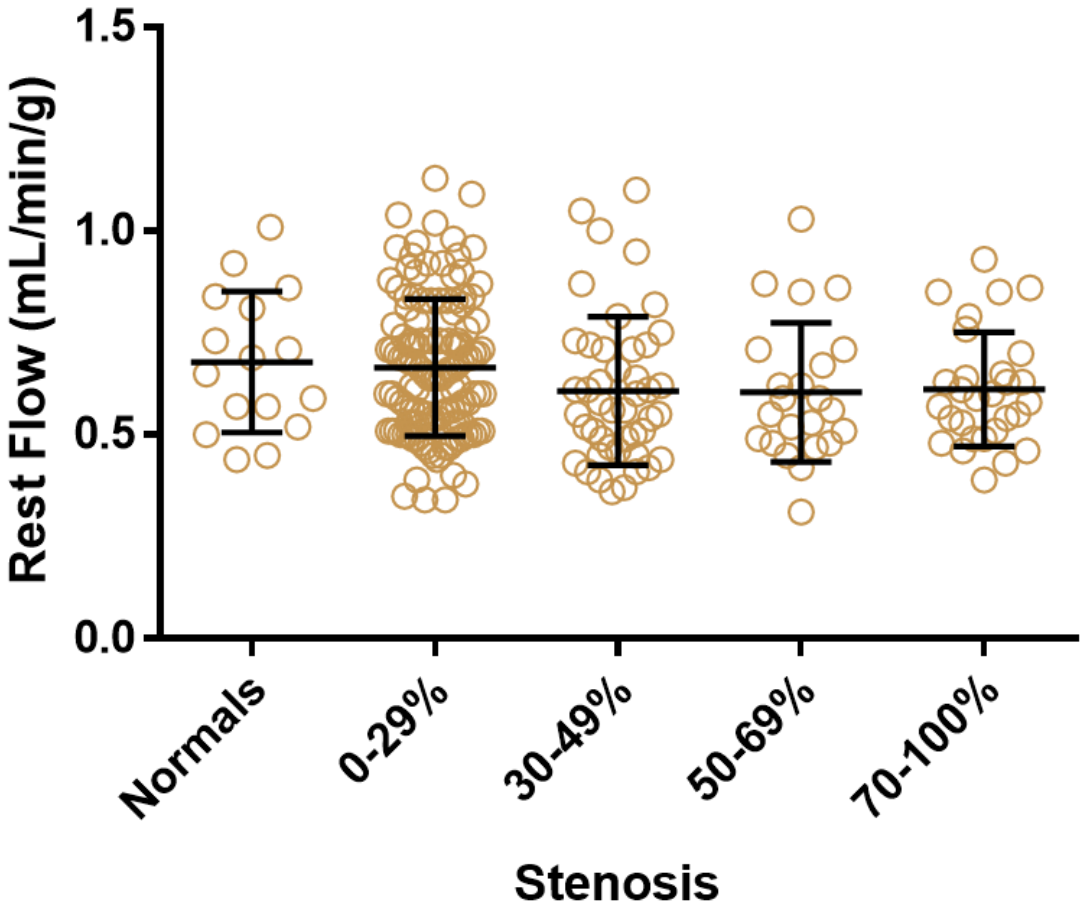

In the LCx territory, there was no significant correlation between segmental rest flow and stenosis burden. The segmental rest flow was 0.68 ± 0.17 $mL*min^{-1}*g^{-1}$ in normals (n=16), 0.66 ± 0.17 in the 0-29% stenosis (n=132), 0.61 ± 0.18 in the 30-49% stenosis (n=45), 0.60 ± 0.17 in the 50-69% stenosis (n=23), and 0.61 ± 0.14 in the 70-100% stenosis (n=29) groups.

Suppl. Figure 1D. Segmental Rest Myocardial Blood Flow and CAD Severity in the RCA.

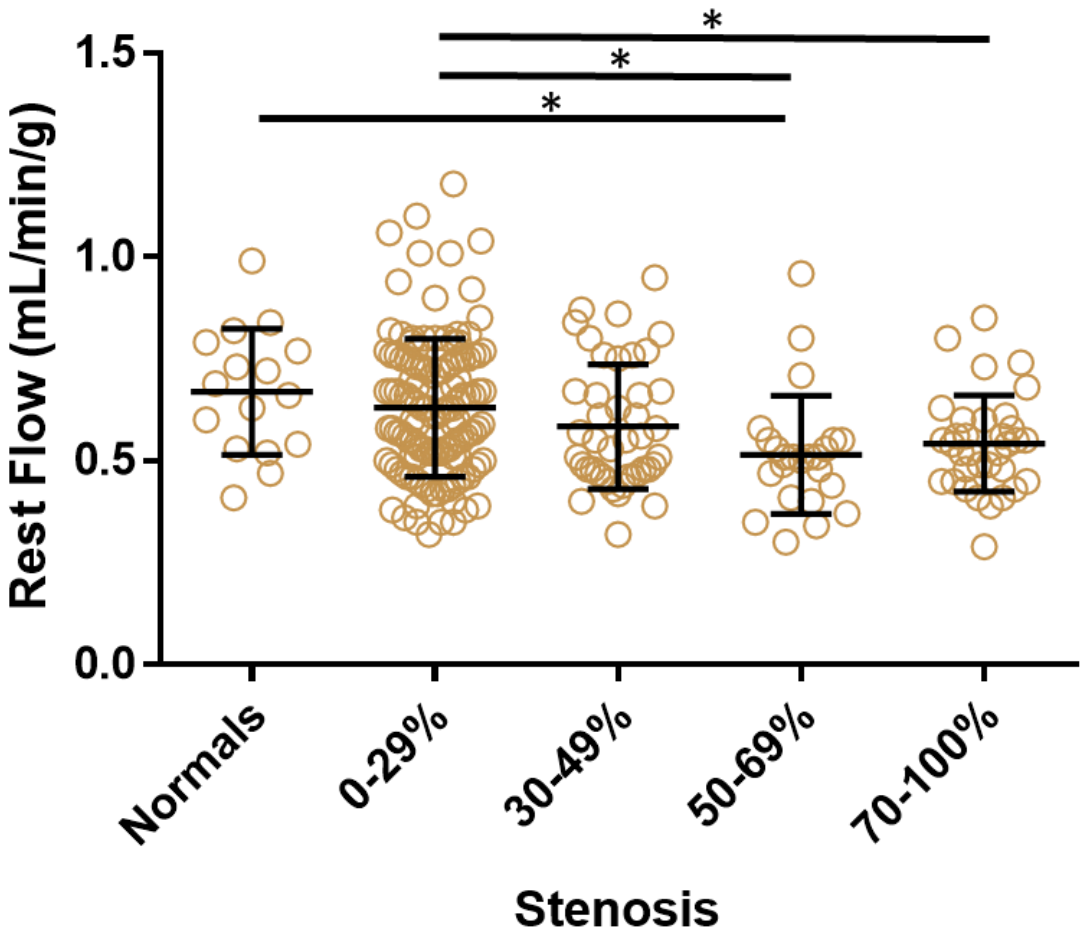

In the RCA territory, there was a marginal correlation between segmental rest flow and stenosis burden. The segmental rest flow was 0.67 ± 0.15 $mL*min^{-1}*g^{-1}$ in normals (n=16), 0.63 ± 0.17 in the 0-29% stenosis (n=128), 0.58 ± 0.15 in the 30-49% stenosis (n=43), 0.51 ± 0.15 in the 50-69% stenosis (n=24), and 0.54 ± 0.12 in the 70-100% stenosis (n=34) groups (*P<0.05).

Suppl. Figure 2A. Segmental Stress Myocardial Blood Flow and CAD Severity in Pooled Coronary Territories.

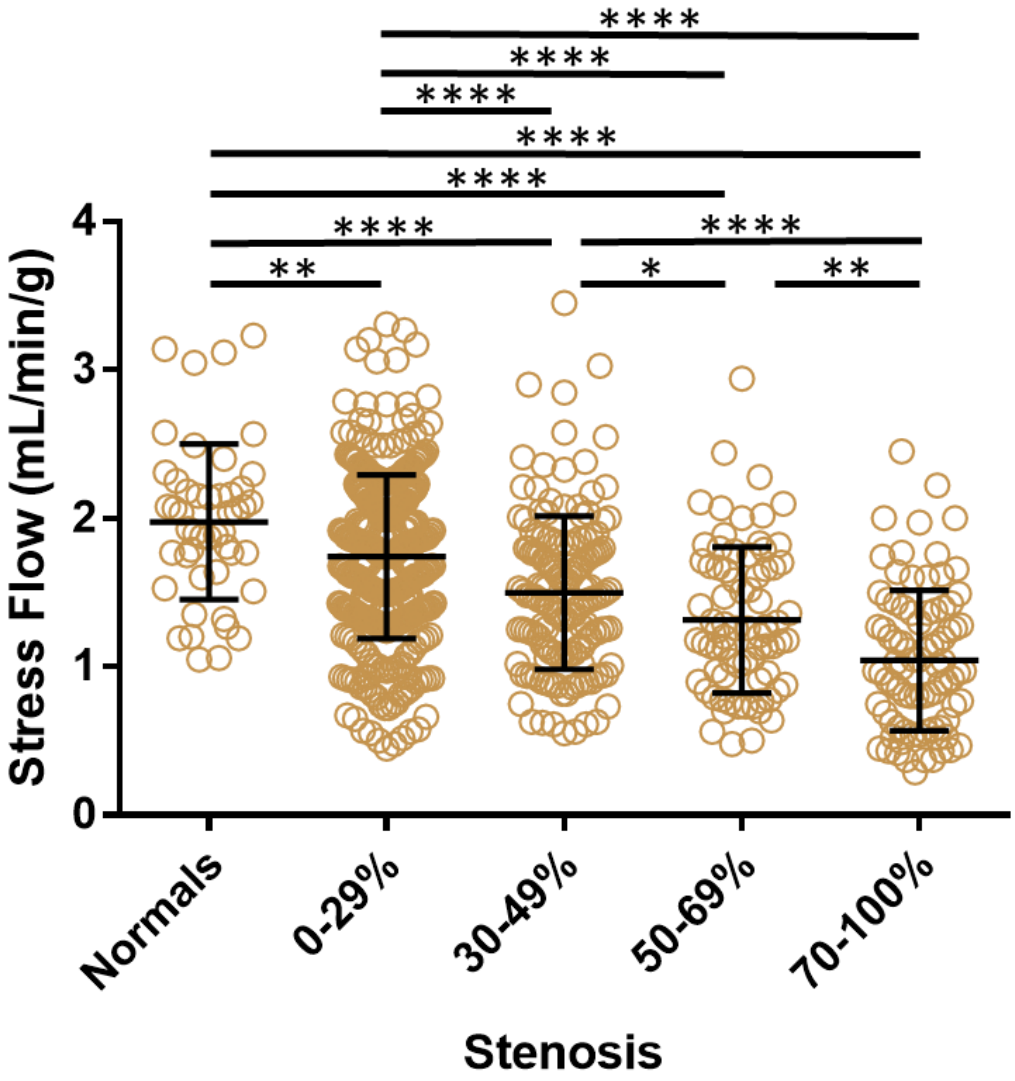

Segmental stress flow had excellent discriminatory ability to detect increasing stenoses in pooled coronary territories, decreasing from 1.98±0.52 $mL*min^{-1}*g^{-1}$ in normals (n=48), to 1.74±0.55 in 0-29% stenosis (n=371), 1.50±0.52 in 30-49% stenosis (n=153), 1.31±0.49 in 50-69% (n=77), and 1.04±0.47 (n=86) in 70-100% stenosis groups (*P<0.05, **P<0.01, ****P<0.0001).

Suppl. Figure 2B. Segmental Stress Myocardial Blood Flow and CAD Severity in the LAD.

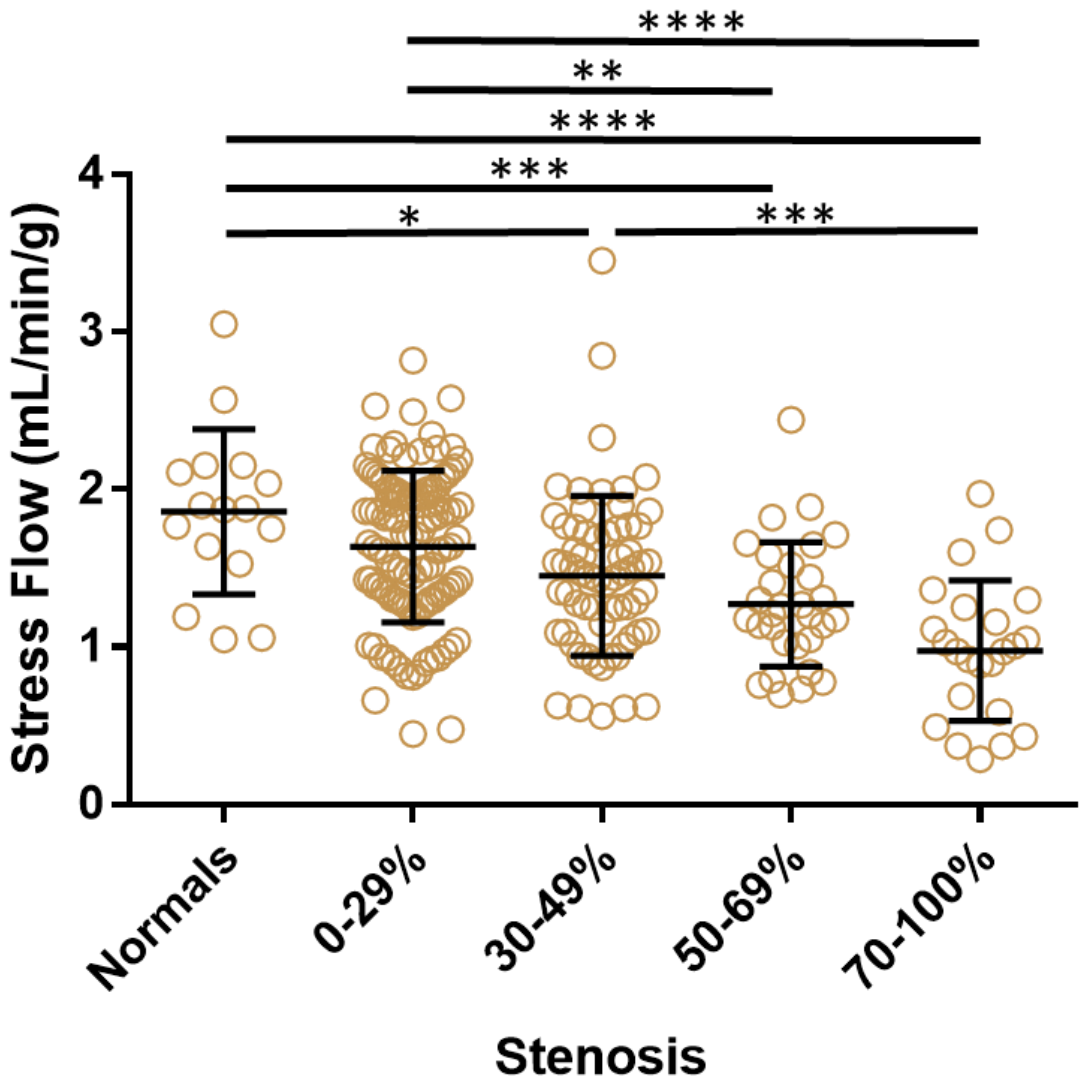

Segmental stress flow significantly correlated with stenosis burden in the LAD territory. The segmental stress flow was 1.86 ± 0.52 $mL*min^{-1}*g^{-1}$ in normals (n=16), 1.64 ± 0.48 in the 0-29% stenosis (n=111), 1.45 ± 0.51 in the 30-49% stenosis (n=65), 1.27 ± 0.40 in the 50-69% stenosis (n=30), and 0.98 ± 0.44 in the 70-100% stenosis (n=23) groups (*P<0.05, **P<0.01, ***P<0.001, ****P<0.0001).

Suppl. Figure 2C. Segmental Stress Myocardial Blood Flow and CAD Severity in the LCx.

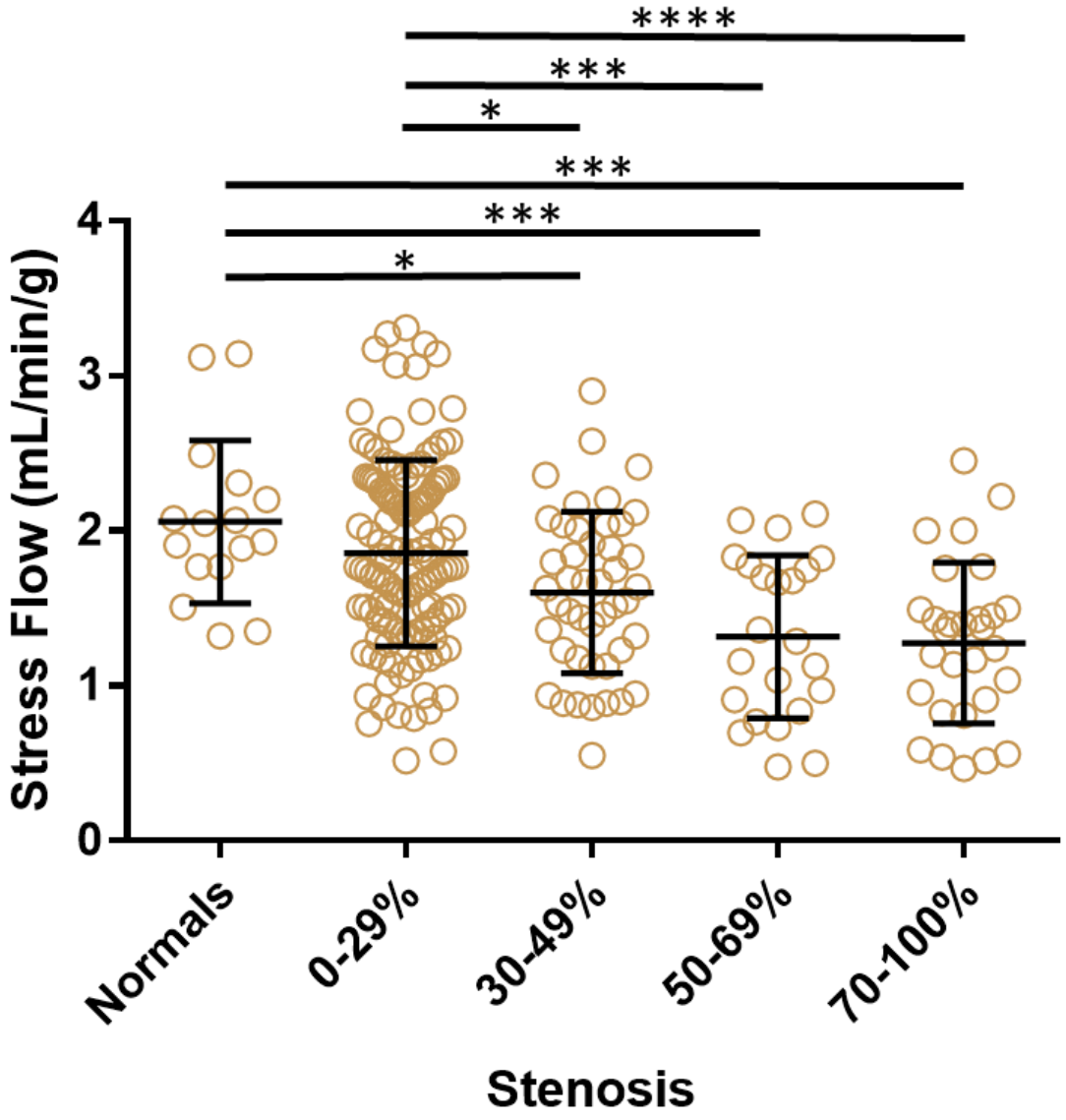

Segmental stress flow significantly correlated with stenosis burden in the LCx territory. The segmental stress flow was 2.06 ± 0.53 $mL*min^{-1}*g^{-1}$ in normals (n=16), 1.86 ± 0.60 in the 0-29% stenosis (n=132), 1.60 ± 0.52 in the 30-49% stenosis (n=45), 1.32 ± 0.52 in the 50-69% stenosis (n=23), and 1.28 ± 0.52 in the 70-100% stenosis (n=29) groups (*P<0.05, ***P<0.001, ****P<0.0001).

Suppl. Figure 2D. Segmental Stress Myocardial Blood Flow and CAD Severity in the RCA.

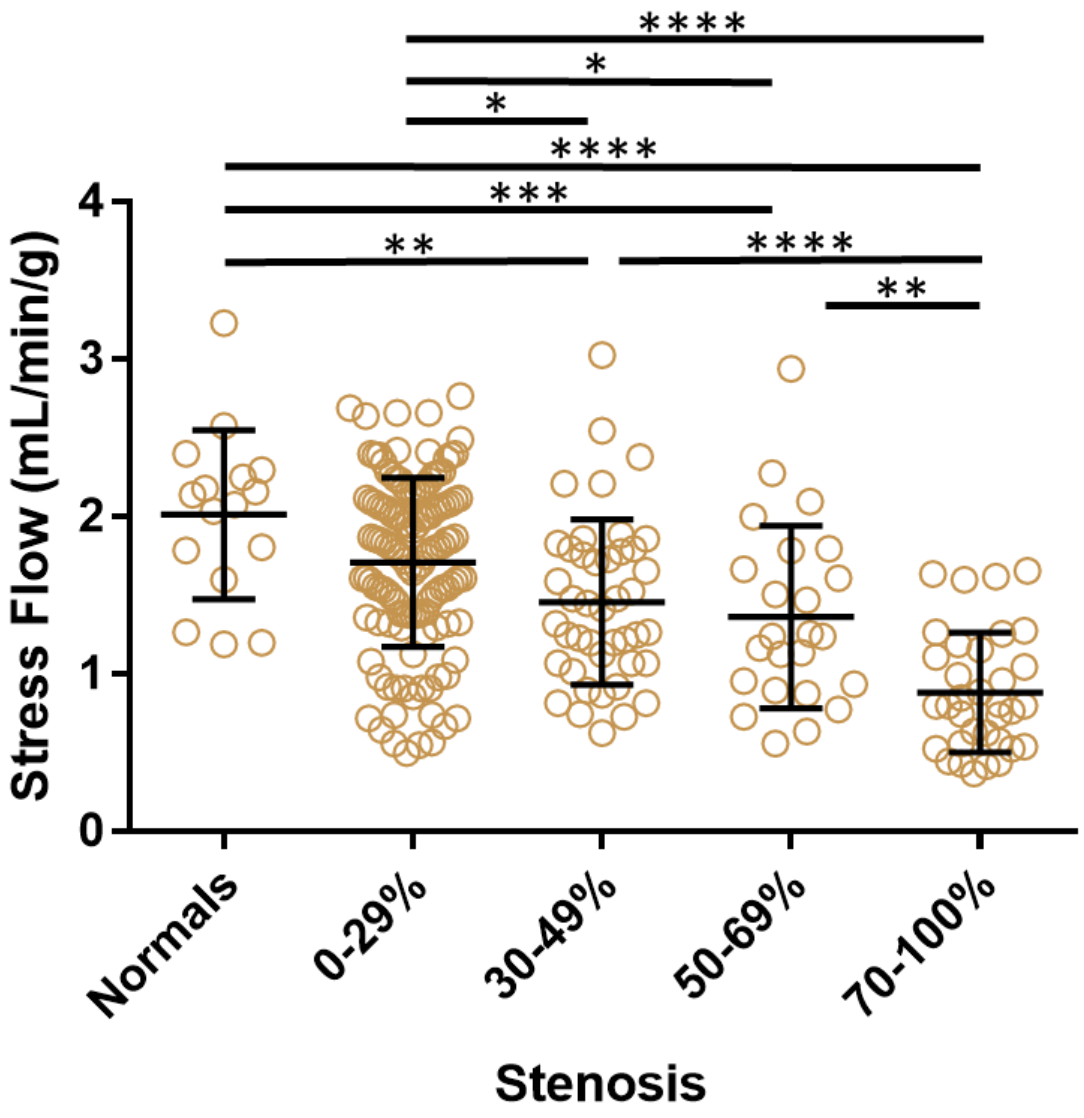

Segmental stress flow significantly correlated with stenosis burden in the RCA territory. The segmental stress flow was 2.01 ± 0.54 $mL*min^{-1}*g^{-1}$ in normals (n=16), 1.71 ± 0.54 in the 0-29% stenosis (n=128), 1.46 ± 0.52 in the 30-49% stenosis (n=43), 1.36 ± 0.58 in the 50-69% stenosis (n=24), and 0.89 ± 0.38 in the 70-100% stenosis (n=34) groups (*P<0.05, **P<0.01, ****P<0.0001).

Suppl. Figure 3A. Segmental Myocardial Flow Reserve and CAD Severity in Pooled Coronary Territories.

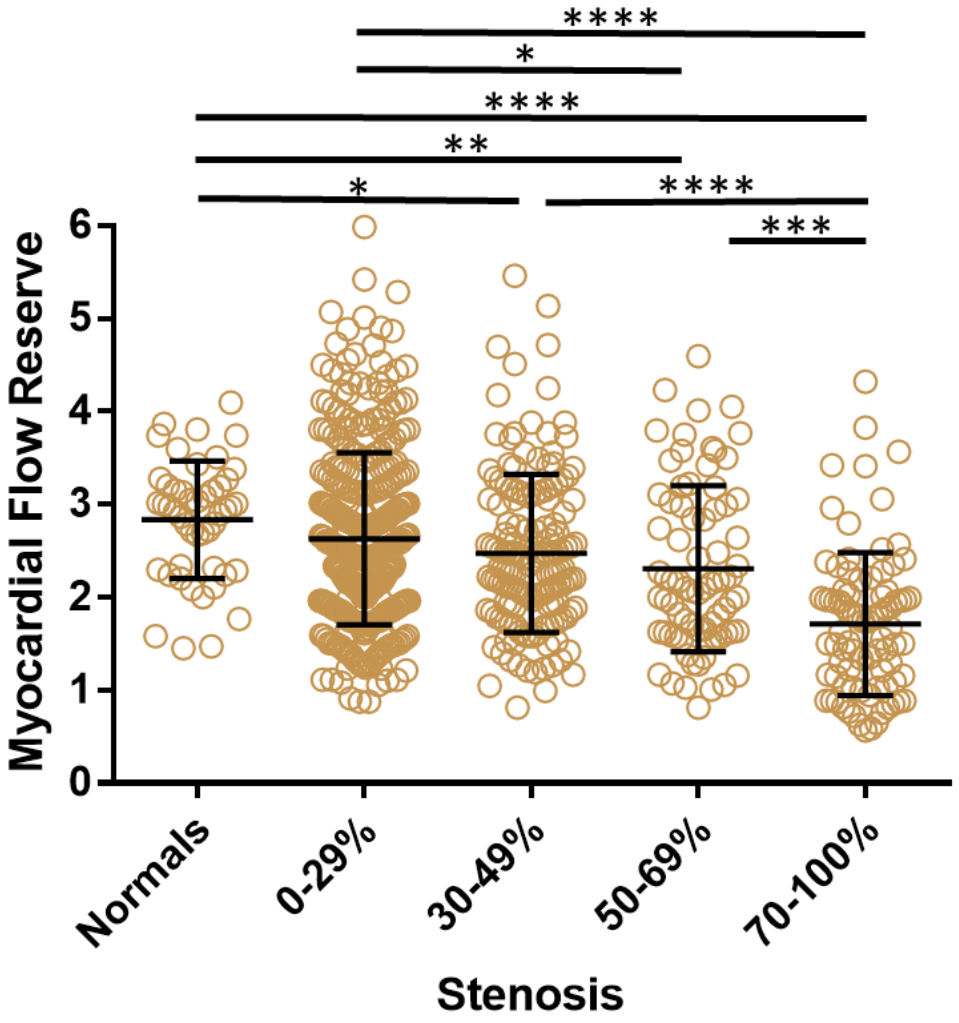

Segmental MFR significantly distinguished increasing CAD stenoses in pooled coronary territories, decreasing from 2.84±0.63 in normals (n=48), to 2.63±0.93 in 0-29% stenosis (n=371), 2.47±0.85 in 30-40% stenosis (n=153), 2.31±0.90 in 50-69% stenosis (n=77), and 1.71±0.77 in 70-100% stenosis (n=86) groups (*P<0.05, **P<0.01, ***P<0.001, ****P<0.0001).

Suppl. Figure 3B. Segmental Myocardial Flow Reserve and CAD Severity in the LAD.

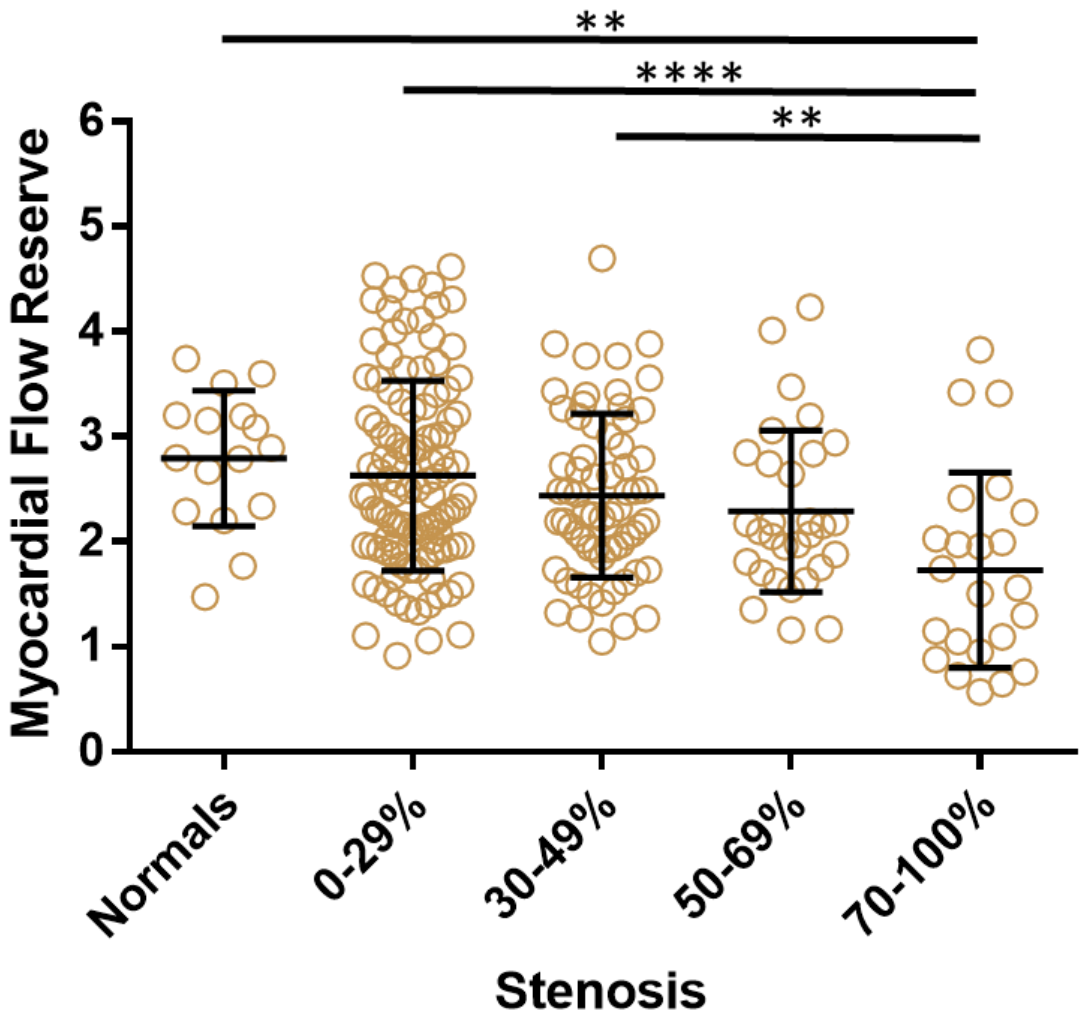

Segmental myocardial flow reserve correlated with stenosis burden in the LAD territory. The segmental myocardial flow reserve was 2.79 ± 0.64 in normals (n=16), 2.63 ± 0.91 in the 0-29% stenosis (n=111), 2.44 ± 0.78 in the 30-49% stenosis (n=65), 2.29 ± 0.77 in the 50-69% stenosis (n=30), and 1.73 ± 0.93 in the 70-100% stenosis (n=23) groups (**P<0.01, ****P<0.0001).

Suppl. Figure 3C. Segmental Myocardial Flow Reserve and CAD Severity in the LCx.

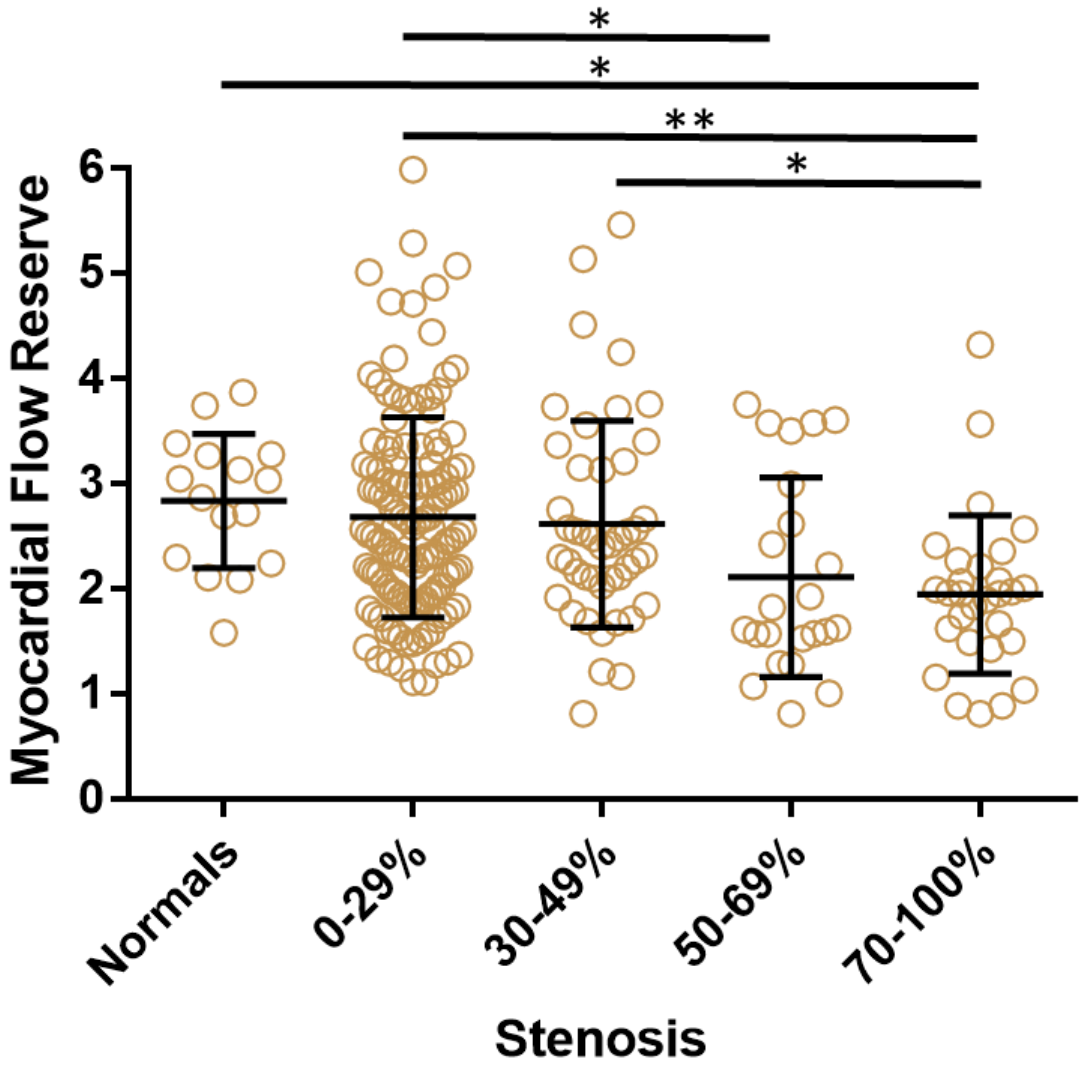

Segmental myocardial flow reserve correlated with stenosis burden in the LCx territory. The segmental myocardial flow reserve was 2.84 ± 0.64 in normals (n=16), 2.68 ± 0.95 in the 0-29% stenosis (n=132), 2.62 ± 0.98 in the 30-49% stenosis (n=45), 2.11 ± 0.95 in the 50-69% stenosis (n=23), and 1.95 ± 0.75 in the 70-100% stenosis (n=29) groups (*P<0.05, **P<0.01).

Suppl. Figure 3D. Segmental Myocardial Flow Reserve and CAD Severity in the RCA.

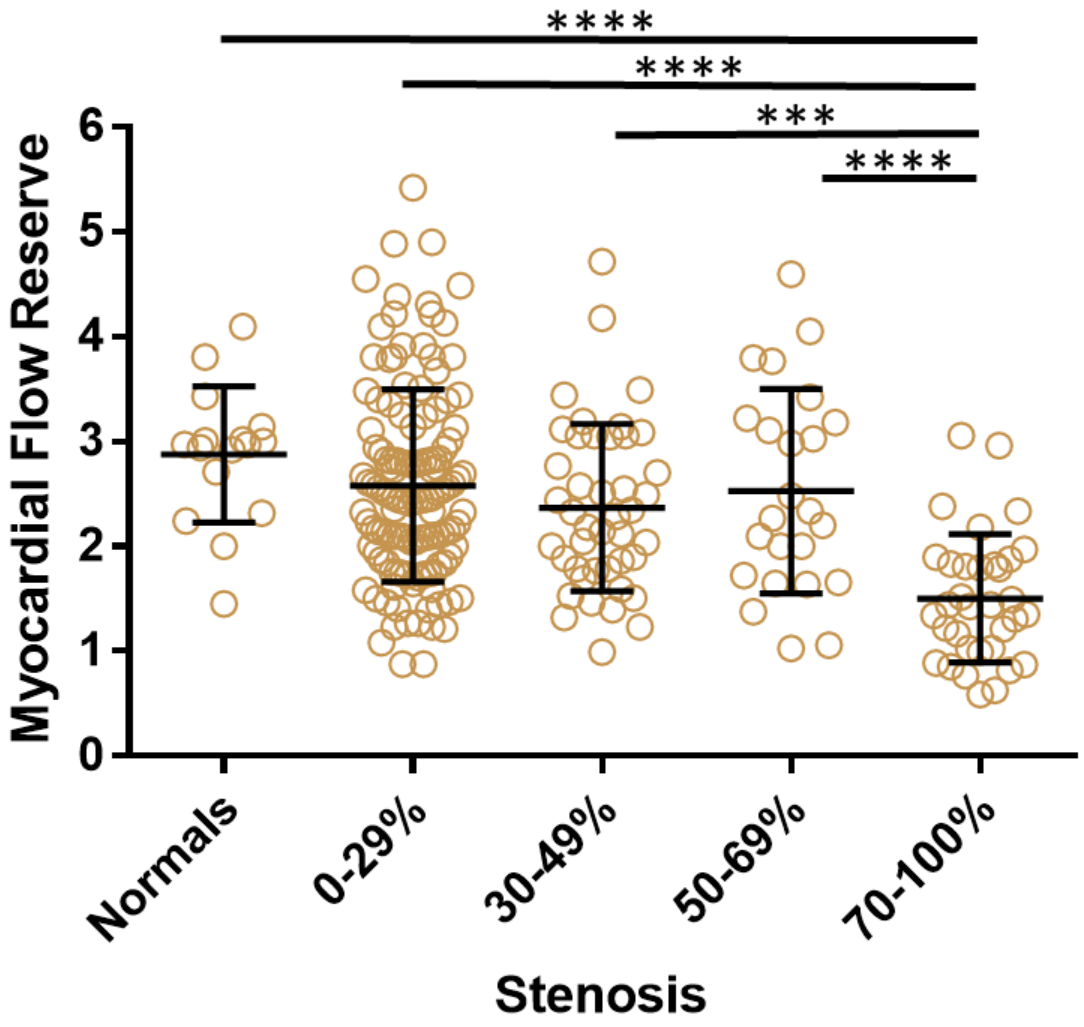

Segmental myocardial flow reserve correlated with stenosis burden in the RCA territory. The segmental myocardial flow reserve was 2.88 ± 0.65 in normals (n=16), 2.58 ± 0.92 in the 0-29% stenosis (n=128), 2.37 ± 0.80 in the 30-49% stenosis (n=43), 2.53 ± 0.98 in the 50-69% stenosis (n=24), and 1.50 ± 0.61 in the 70-100% stenosis (n=34) groups (***P<0.001, ****P<0.0001).

Suppl. Figure 4A. Segmental Relative Flow Reserve and CAD Severity in Pooled Coronary Territories.

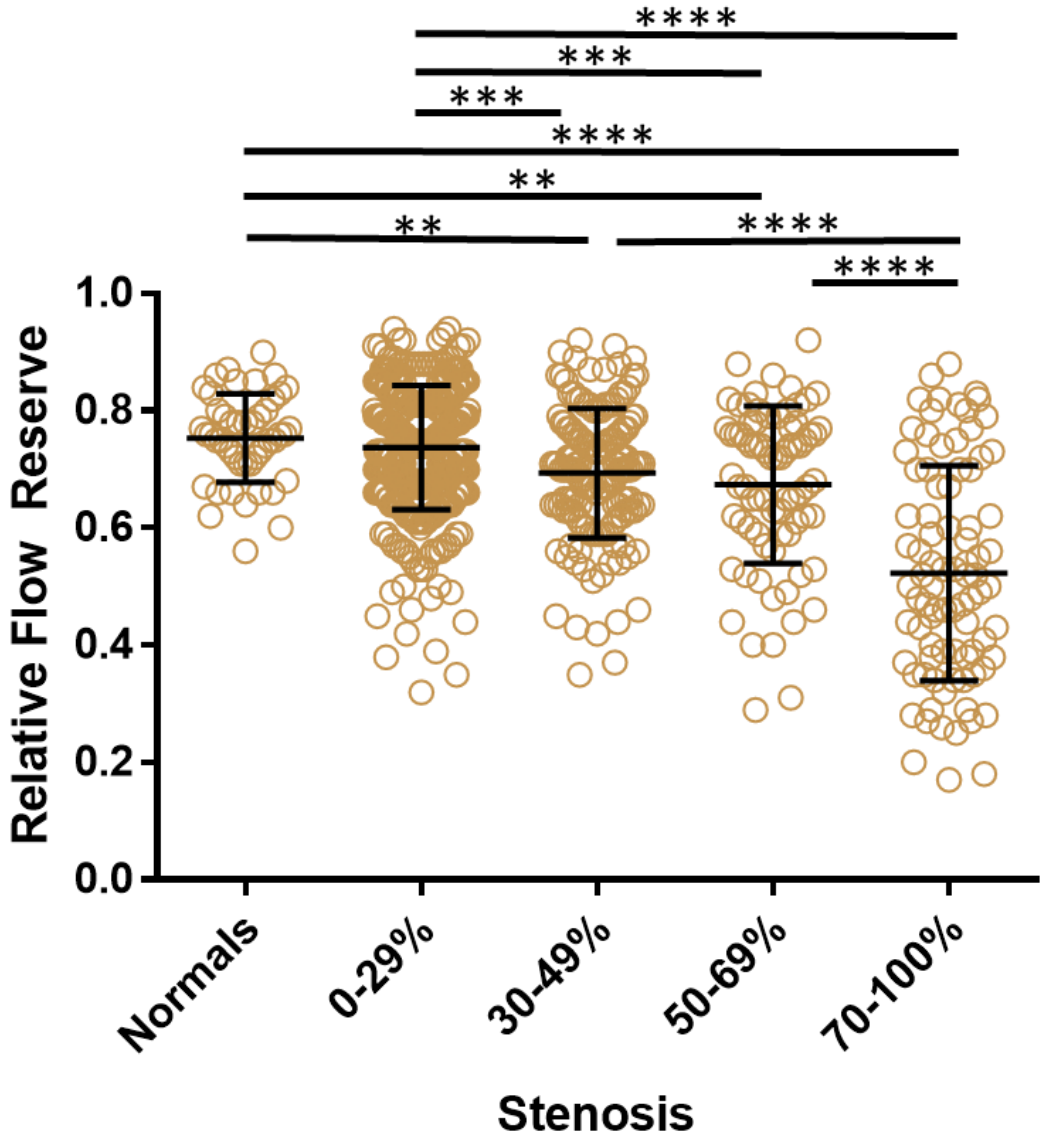

Segmental RFR significantly distinguished increasing CAD stenoses in pooled coronary territories, decreasing from 0.75±0.08 in normals (n=48), to 0.74±0.11 in 0-29% stenosis (n=371), 0.69±0.11 in 30-40% stenosis (n=153), 0.67±0.13 in 50-69% stenosis (n=77), and 0.52±0.18 in 70-100% stenosis (n=86) groups (**P<0.01, ***P<0.001, ****P<0.0001).

Suppl. Figure 4B. Segmental Relative Flow Reserve and CAD Severity in the LAD.

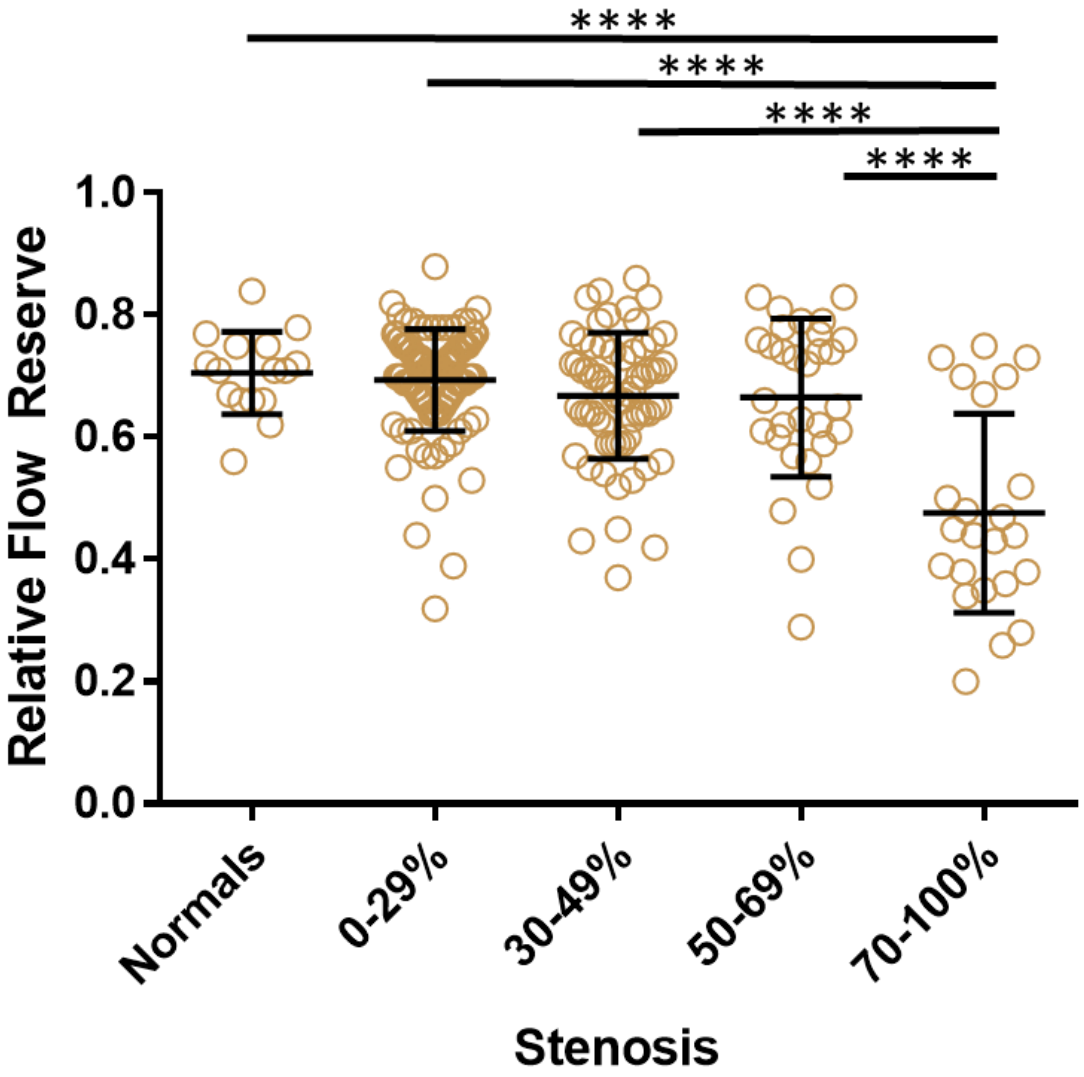

Segmental relative flow reserve in the LAD territory significantly decreased in the 70-100% stenosis group. The segmental relative flow reserve was 0.71 ± 0.07 in normals (n=16), 0.69 ± 0.08 in the 0-29% stenosis (n=111), 0.67 ± 0.10 in the 30-49% stenosis (n=65), 0.67 ± 0.13 in the 50-69% stenosis (n=30), and 0.48 ± 0.16 in the 70-100% stenosis (n=23) groups (****P<0.0001).

Suppl. Figure 4C. Segmental Relative Flow Reserve and CAD Severity in the LCx.

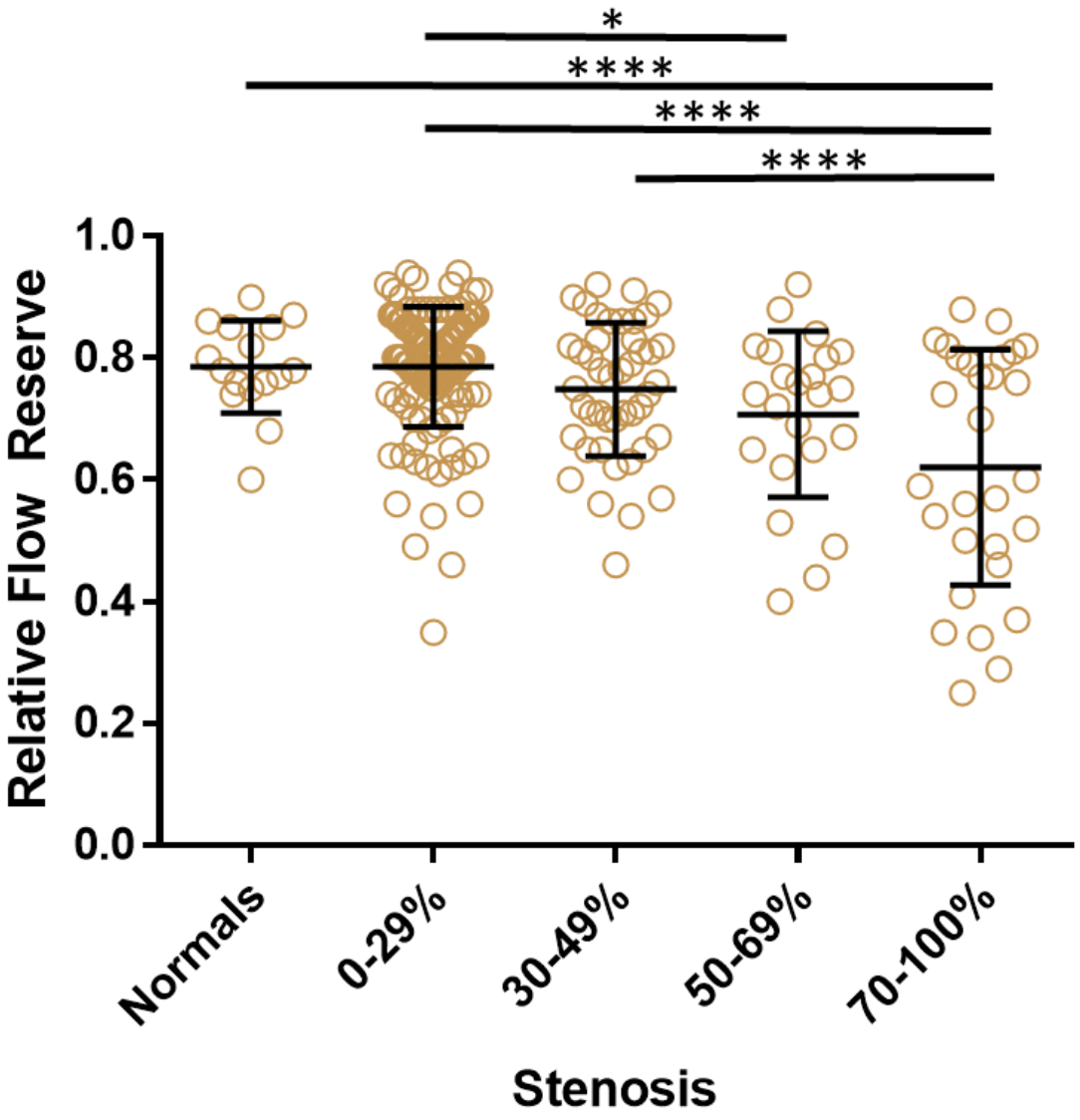

Segmental relative flow reserve correlated with stenosis burden in the LCx territory. The segmental relative flow reserve was 0.79 ± 0.08 in normals (n=16), 0.79 ± 0.10 in the 0-29% stenosis (n=132), 0.75 ± 0.11 in the 30-49% stenosis (n=45), 0.71 ± 0.14 in the 50-69% stenosis (n=23), and 0.62 ± 0.19 in the 70-100% stenosis (n=29) groups (*P<0.05, ****P<0.0001).

Suppl. Figure 4D. Segmental Relative Flow Reserve and CAD Severity in the RCA.

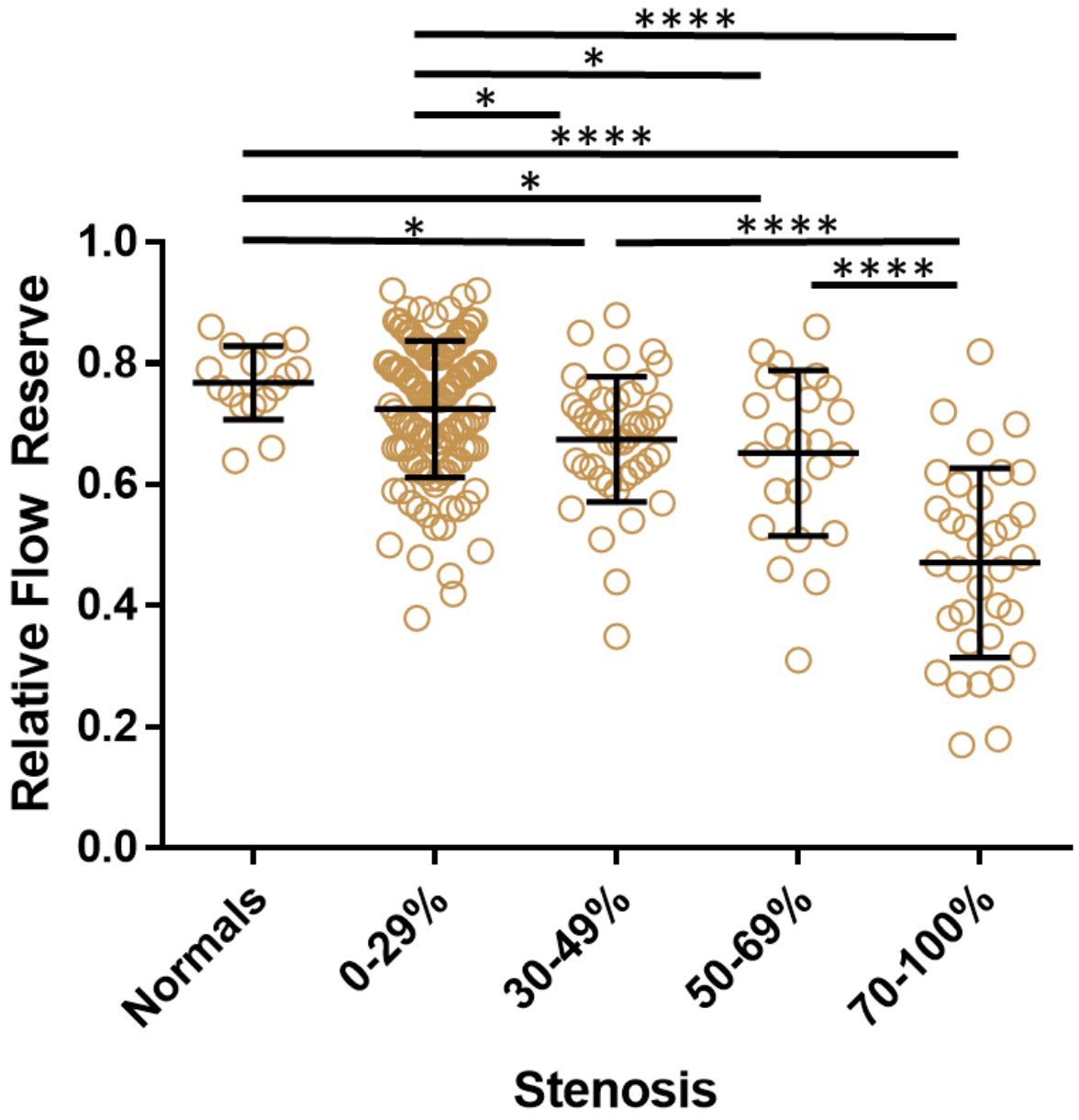

Segmental relative flow reserve correlated with stenosis burden in the RCA territory. The segmental relative flow reserve was 0.77 ± 0.06 in normals (n=16), 0.72 ± 0.11 in the 0-29% stenosis (n=128), 0.67 ± 0.10 in the 30-49% stenosis (n=43), 0.65 ± 0.14 in the 50-69% stenosis (n=24), and 0.47 ± 0.16 in the 70-100% stenosis (n=34) groups (*P<0.05, ****P<0.0001).

Suppl. Figure 5A. Per-Vessel Diagnostic Performance of Perfusion Quantitation, Segmental, and Territory Flow Metrics for CAD ≥50% Categorization.

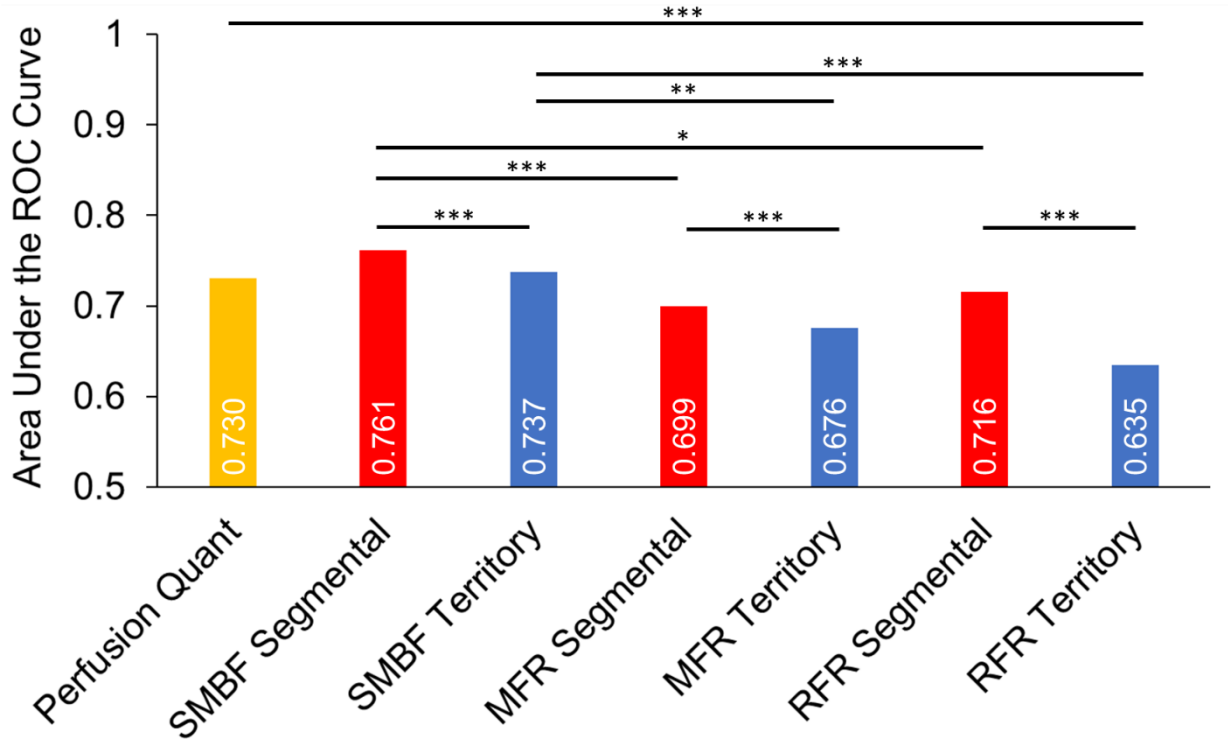

Bar graph depiction of Figure 3A. For CAD ≥50% categorization of pooled coronary territories (n=735), we conducted 3 sets of analyses. First, the perfusion quantitation AUC=0.730 (0.686-0.775) was significantly greater than the RFR territory AUC=0.635 (0.582-0.688), but not any of the other flow parameters. Second, all the segmental flow metrics demonstrated significantly greater diagnostic performance than their territory counterparts (segmental SMBF AUC=0.761 [0.720-0.802] vs. territory SMBF AUC=0.737 [0.695-0.779]; segmental MFR AUC=0.699 [0.651-0.748] vs. territory MFR AUC=0.676 [0.627-0.725]; segmental RFR AUC=0.716 [0.666-0.765] vs. territory RFR AUC=0.635 [0.582-0.688]). Third, we assessed the diagnostic performance of the 3 flow parameters

compared to each other. Whereas segmental stress MBF was significantly superior to segmental MFR and to segmental RFR, as was territory stress MBF to territory MFR and to territory RFR, there was no significant difference between segmental MFR and segmental RFR, or territory MFR and territory RFR (*P<0.05, **P<0.01, ***P<0.001).

Suppl. Figure 5B. Diagnostic Performance of Segmental vs. Territory Stress Flow for CAD ≥50% Categorization by Coronary Territory.

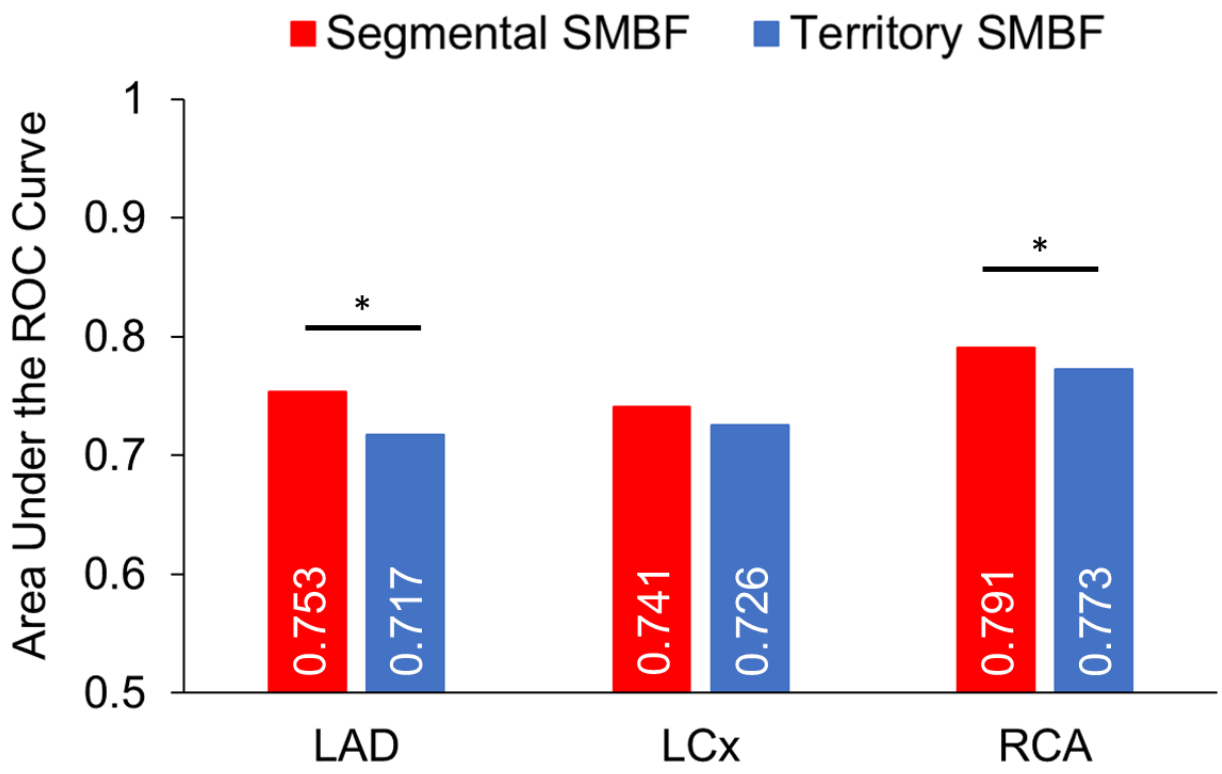

For the CAD ≥50% categorization of individual coronary territories (n=245), the LAD segmental stress flow AUC=0.753 (0.683-0.824) was significantly greater than the LAD territory stress flow AUC=0.717 (0.644-0.791) (*P<0.05). Similarly, the RCA segmental stress flow AUC=0.791 (0.723-0.858) was significantly greater than the RCA territory stress flow AUC=0.773 (0.705-0.840) (*P<0.05). The LCx segmental stress flow AUC=0.741 (0.667-0.814) was numerically greater than the LCx territory stress MBF AUC=0.726 (0.652-0.799) however not statistically significant.

Suppl. Figure 5C. Diagnostic Performance of Segmental vs. Territory Myocardial Flow Reserve for CAD ≥50% Categorization by Coronary Territory.

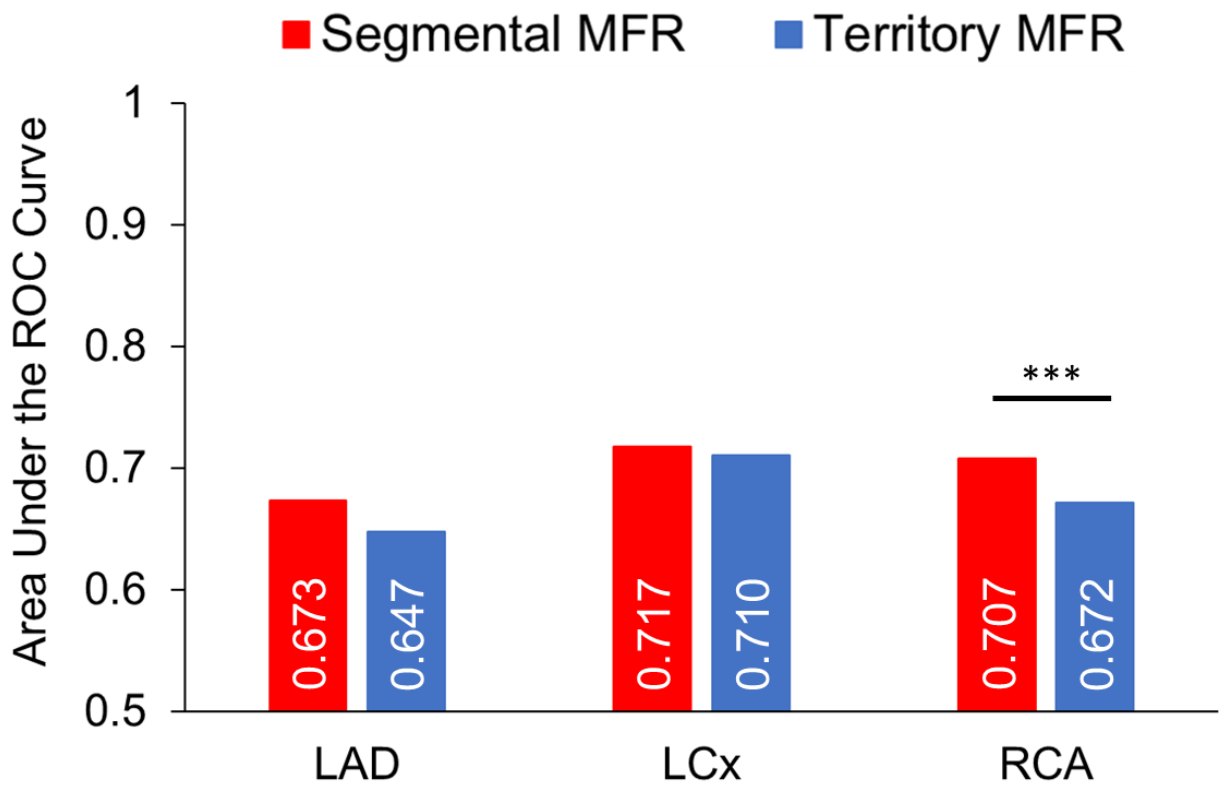

For the CAD ≥50% categorization of individual coronary territories (n=245), the RCA segmental MFR AUC=0.707 (0.623-0.791) was significantly greater than the RCA territory MFR AUC=0.672 (0.586-0.757) (***P<0.001). The LAD segmental MFR AUC=0.673 (0.588-0.759) was numerically greater than the LAD territory MFR AUC=0.647 (0.558-0.736) however not statistically significant. The LCx segmental MFR AUC=0.717 (0.634-0.800) was similar to the LCx territory MFR AUC=0.710 (0.627-0.793).

Suppl. Figure 6A. Per-Vessel Diagnostic Performance of Perfusion Quantitation, Segmental, and Territory Flow Metrics for CAD ≥70% Categorization.

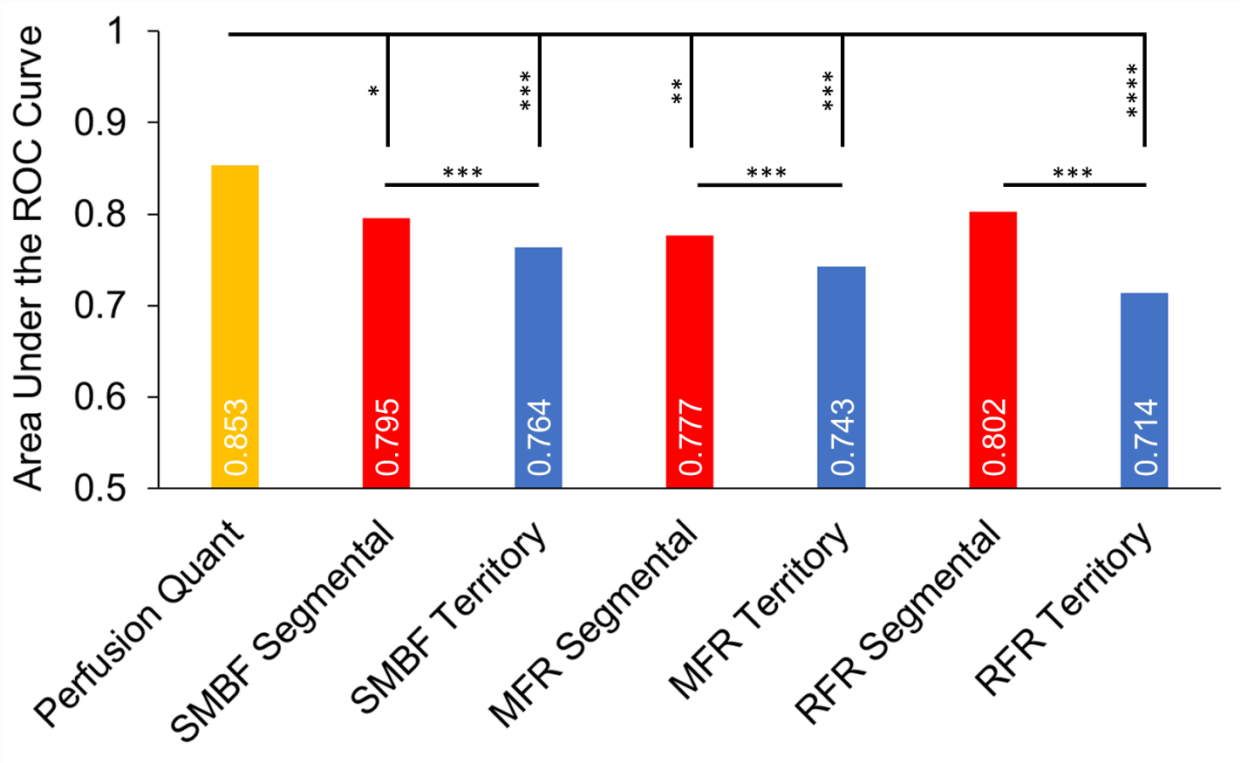

Bar graph depiction of Figure 3B. For CAD ≥70% categorization of pooled coronary territories (n=735), we conducted 3 sets of analyses. First, the perfusion quantitation AUC=0.853 (0.809-0.897) was significantly greater than all the flow metrics other than segmental RFR AUC=0.802 (0.741-0.863). Second, all the segmental flow metrics demonstrated significantly greater diagnostic performance than their territory counterparts (segmental SMBF AUC=0.795 [0.746-0.844] vs. territory SMBF AUC=0.764 [0.712-0.816]; segmental MFR AUC=0.777 [0.723-0.831] vs. territory MFR AUC=0.743 [0.687-0.799]; segmental RFR AUC=0.802 [0.741-0.863] vs. territory RFR AUC=0.714 [0.643-0.785]). The diagnostic performances of SMBF, MFR, and RFR flow parameters

were not significantly different from each other (*P<0.05, **P<0.01, ***P<0.001, ****P<0.0001).

Suppl. Figure 6B. Diagnostic Performance of Segmental vs. Territory Stress Flow for CAD ≥70% Categorization by Coronary Territory.

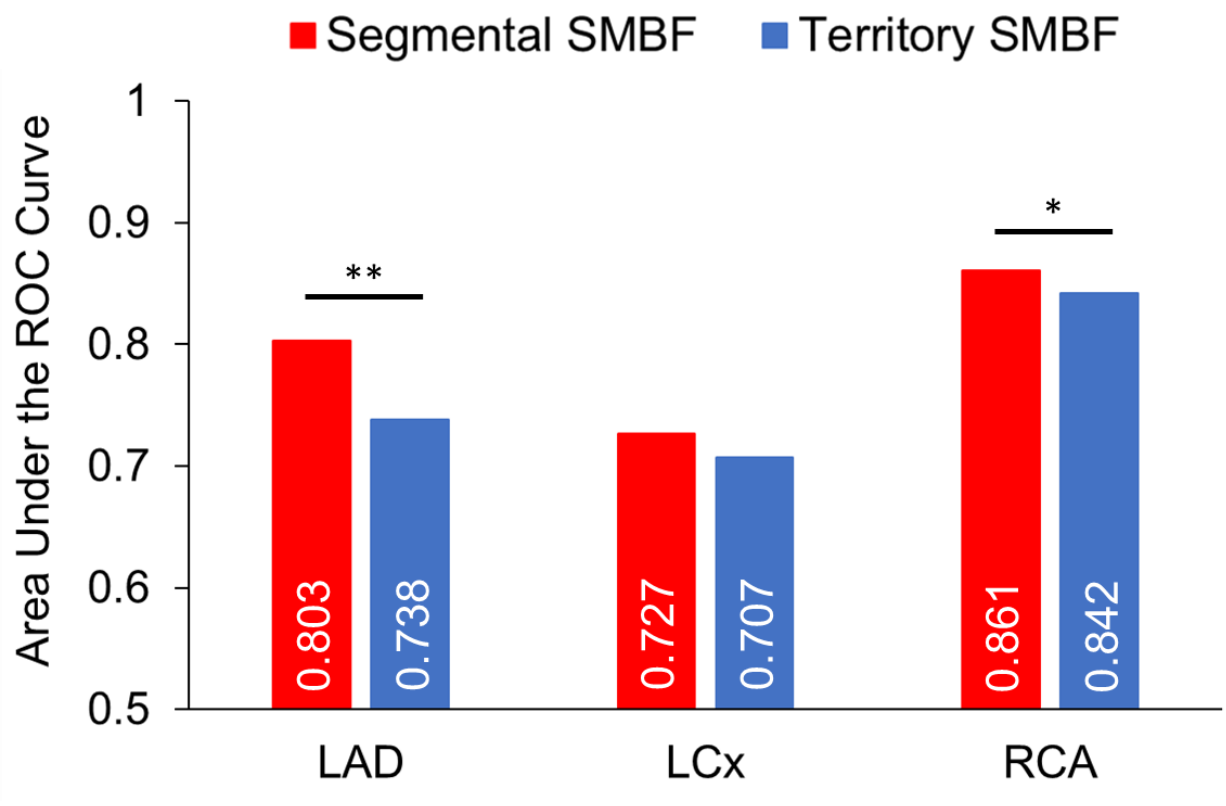

For the CAD ≥70% categorization of individual coronary territories (n=245), the LAD segmental stress flow AUC=0.803 (0.711-0.896) was significantly greater than the LAD territory stress flow AUC=0.738 (0.630-0.846) (**P<0.01). Similarly, the RCA segmental stress flow AUC=0.861 (0.802-0.920) was significantly greater than the RCA territory stress flow AUC=0.842 (0.781-0.903) (*P<0.05). The LCx segmental stress flow AUC=0.727 (0.633-0.821) was numerically greater than the LCx territory stress MBF AUC=0.707 (0.615-0.800) however not statistically significant.

Suppl. Figure 6C. Diagnostic Performance of Segmental vs. Territory Myocardial Flow Reserve for CAD ≥70% Categorization by Coronary Territory.

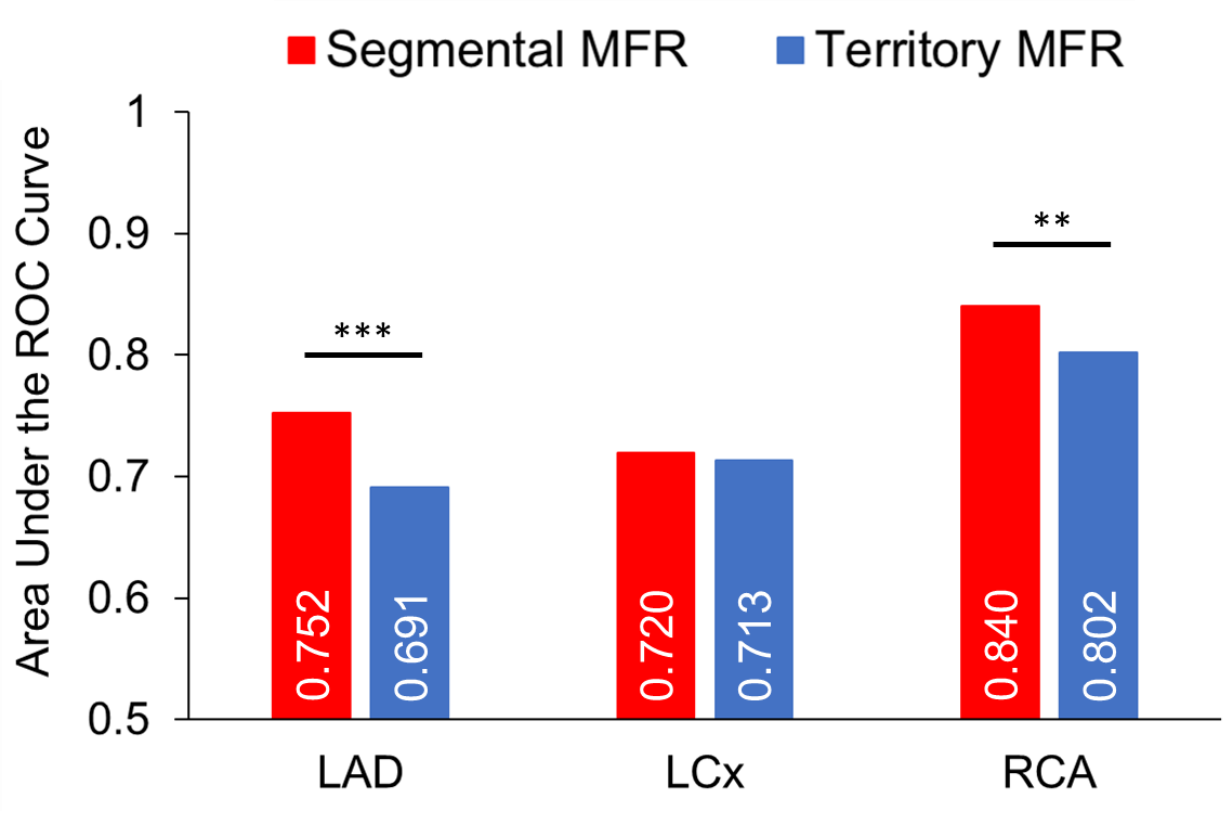

For the CAD ≥70% categorization of individual coronary territories (n=245), the LAD segmental MFR AUC=0.752 (0.628-0.876) was significantly greater than the LAD territory MFR AUC=0.691 (0.554-0.828) (**P<0.01). Similarly, the RCA segmental MFR AUC=0.840 (0.770-0.911) was significantly greater than the RCA territory MFR AUC=0.802 (0.728-0.876). The LCx segmental MFR AUC=0.720 (0.627-0.814) was similar to the LCx territory MFR AUC=0.713 (0.621-0.806) (**P<0.01).

Suppl. Fig. 7A. Diagnostic Performance of the Lowest 1 Segment vs. 2 Segments in the LAD Territory for CAD ≥50% Categorization.

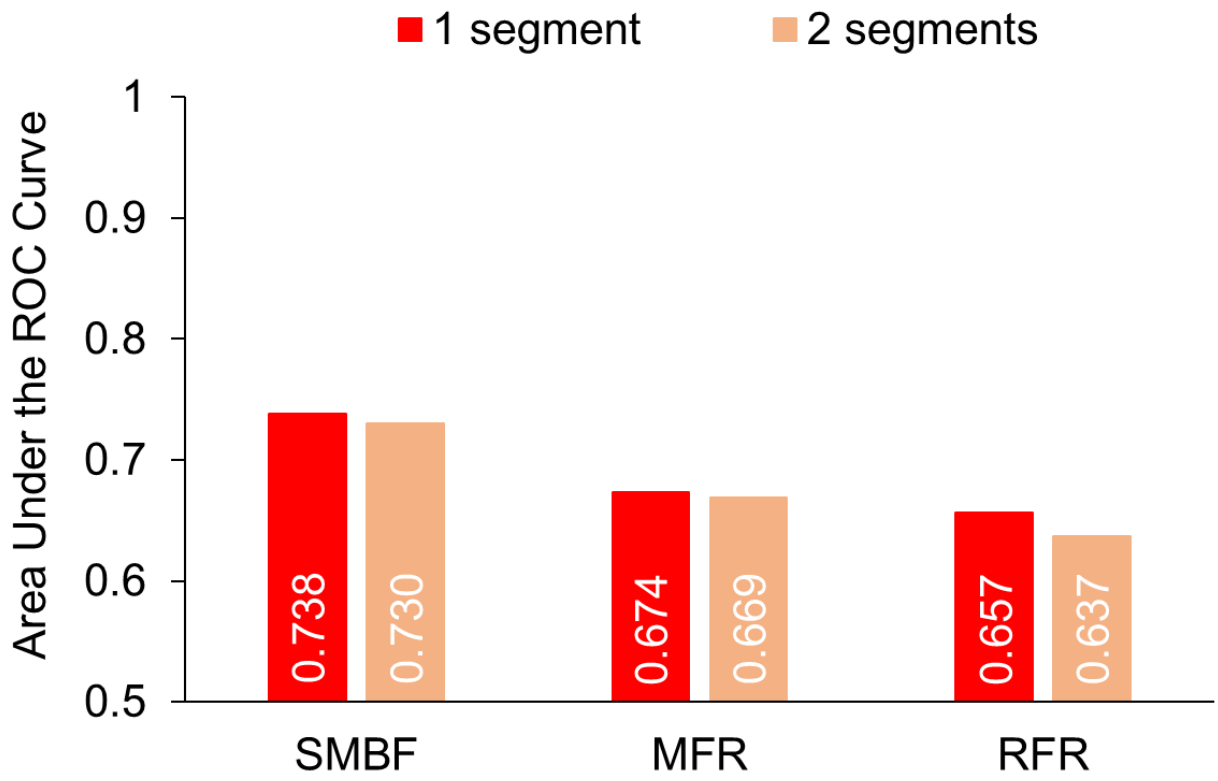

There was no significant difference in diagnostic performance of flow metrics between the lowest 1-segment compared to 2-segment analyses in the LAD territory. The 1- vs. 2-segment AUC's were 0.738 (0.664-0.811) and 0.730 (0.657-0.804) for SMBF; 0.674 (0.588-0.759) and 0.669 (0.581-0.756) for MFR; 0.657 (0.557-0.757) and 0.637 (0.536-0.737) for RFR, respectively (n=245).

Suppl. Fig. 7B. Diagnostic Performance of the Lowest 1 Segment vs. 2 Segments in the LAD territory for CAD ≥70% Categorization.

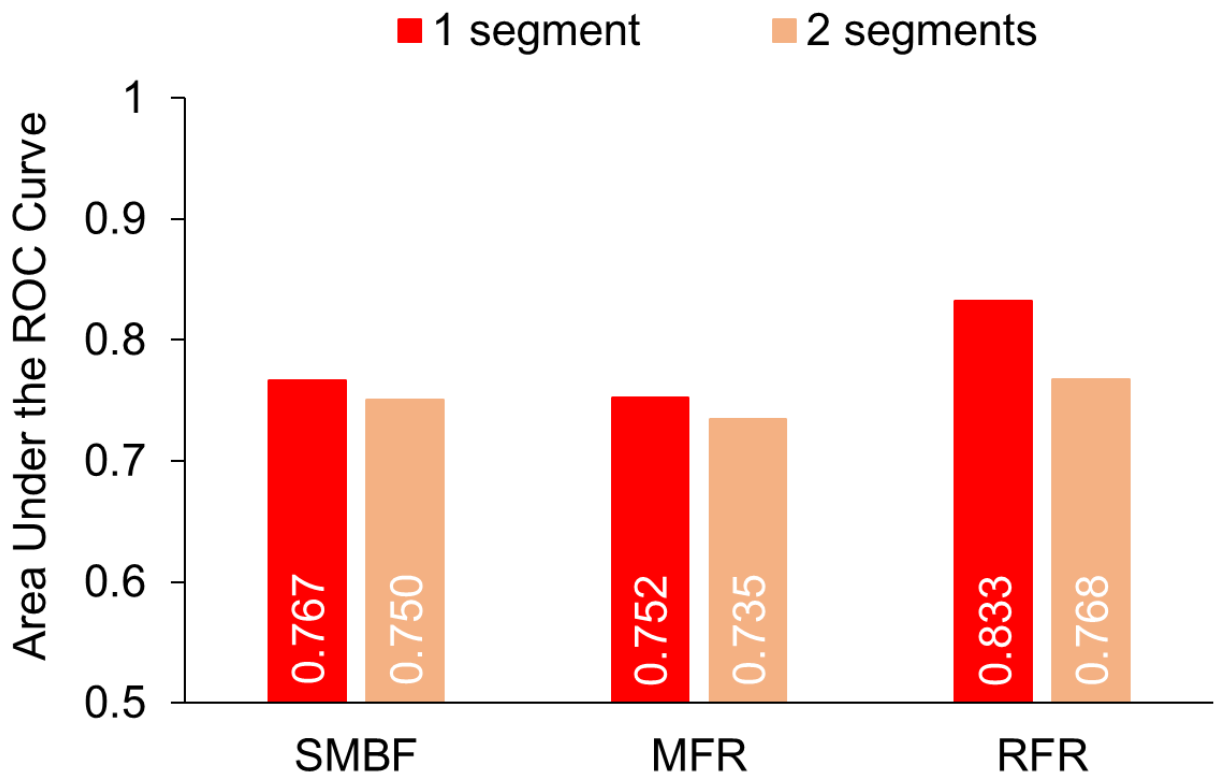

There was no significant difference in diagnostic performance of flow metrics between the lowest 1-segment compared to 2-segment analyses in the LAD territory. The 1- vs. 2-segment AUC's were 0.767 (0.660-0.874) and 0.750 (0.640-0.861) for SMBF; 0.752 (0.629-0.876) and 0.735 (0.602-0.868) for MFR; 0.833 (0.725-0.940) and 0.768 (0.625-0.910) for RFR, respectively (n=245).

Suppl. Figure 8. Per-Vessel Diagnostic Performance of Perfusion Quantitation, Segmental, and Territory Flow Metrics for CAD 50-69% Categorization.

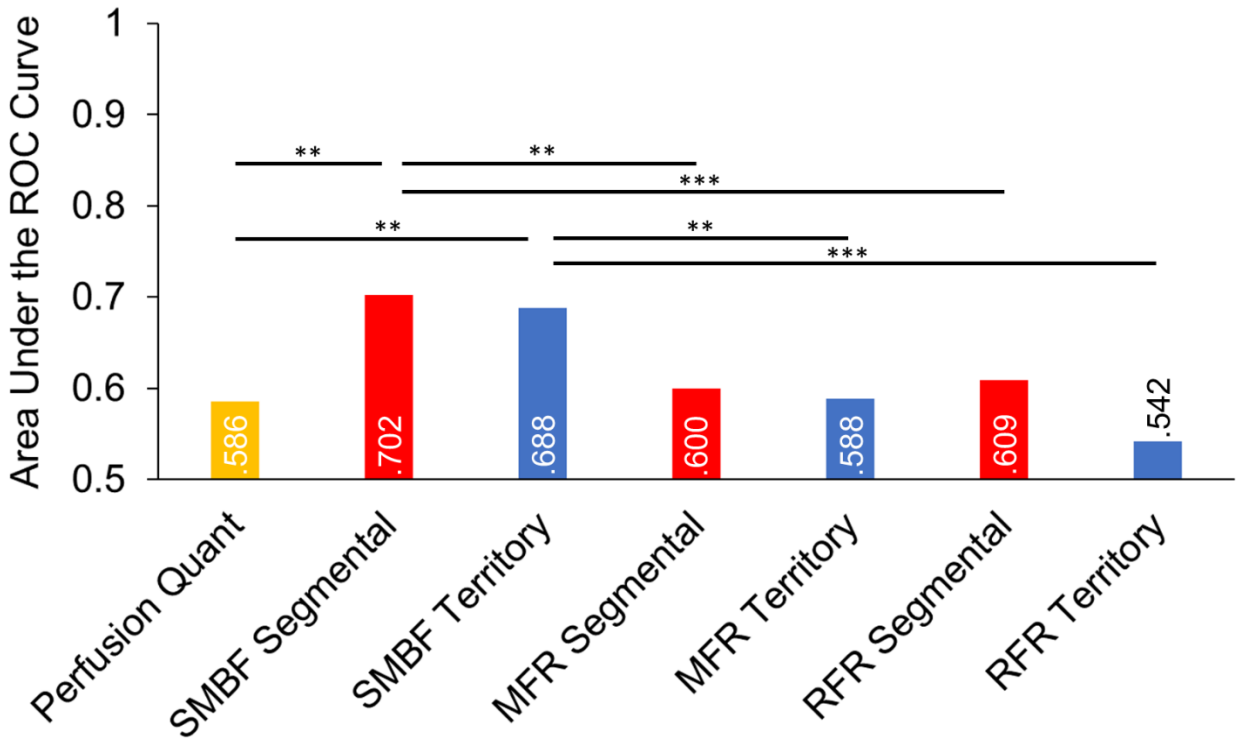

For CAD 50-69% categorization of pooled coronary territories (n=649), the perfusion quantitation AUC=0.586 (0.522-0.649) was significantly inferior to both the segmental SMBF AUC=0.702 (0.642-0.763) and the territory SMBF AUC=0.688 (0.629-0.747), but not significantly different from other flow parameters. The segmental SMBF AUC=0.702 (0.642-0.763) was superior to both the segmental MFR AUC=0.600 (0.528-0.673) and the segmental RFR AUC=0.609 (0.539-0.678). Similarly, the territory SMBF AUC=0.688 (0.629-0.747) was superior to both the territory MFR AUC=0.588 (0.515-0.662) and the territory RFR AUC=0.542 (0.471-0.613) (**P<0.01, ***P<0.001).

Suppl. Figure 9A. Per-Vessel Diagnostic Performance of Perfusion Quantitation, Segmental, and Territory Flow Metrics for CAD 70-79% Categorization.

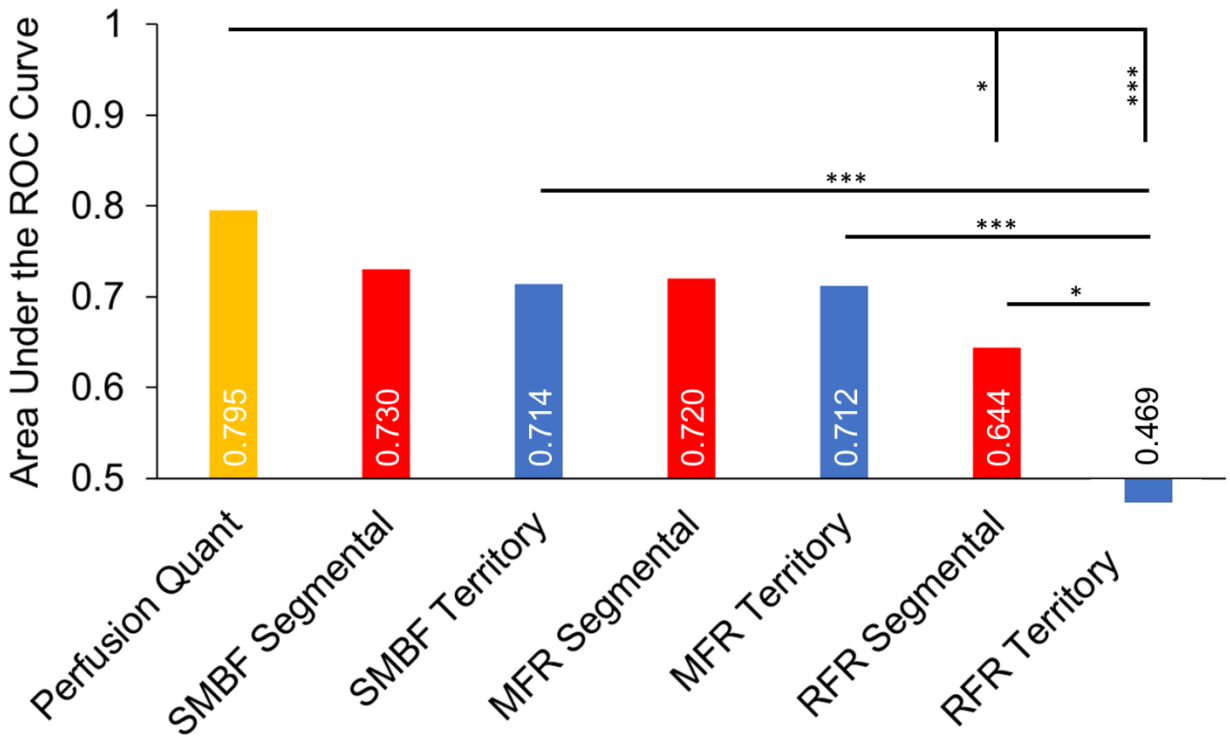

For CAD 70-79% categorization of pooled coronary territories (n=664), we conducted 3 sets of analyses. First, perfusion quantitation was compared with flow metrics. The perfusion quantitation AUC=0.795 (0.695-0.895) was similar to SMBF and MFR metrics and significantly greater only than the segmental RFR AUC=0.644 (0.487-0.801) and the territory RFR AUC=0.469 (0.321-0.617). Second, segmental and territory flow metrics were compared with each other. Segmental SMBF (AUC=0.730 [0.634-0.826] was similar to territory SMBF (AUC=0.714 [0.623- 0.806], as was segmental MFR (AUC=0.720 [0.621- 0.818] to territory MFR (AUC= 0.712 [0.619-0.804]. Segmental RFR however was superior to territory RFR. When comparing the diagnostic performances of SMBF, MFR,

and RFR flow parameters with each other, territory RFR faired significantly worse than territory MFR and territory SMBF (*P<0.05, ***P<0.001).

Suppl. Figure 9B. Per-Vessel Diagnostic Performance of Combinatorial Perfusion Quantitation and Flow Metrics for CAD 70-79% Categorization.

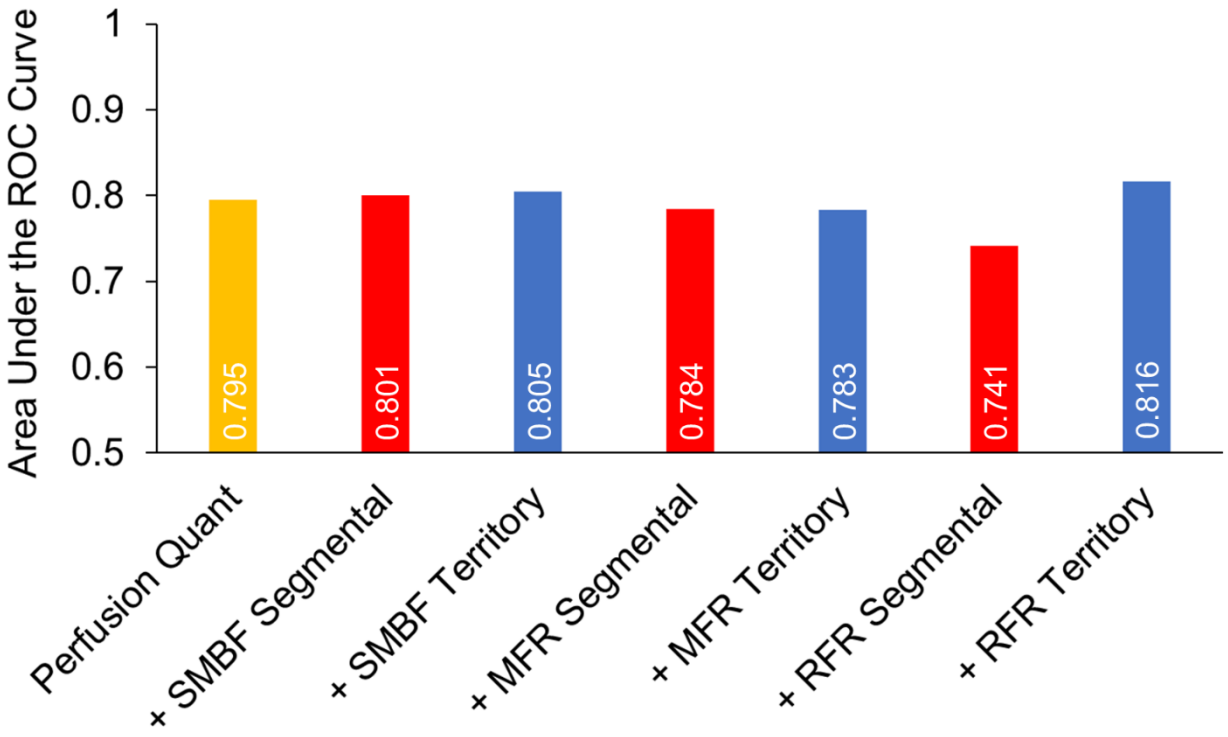

For CAD 70-79% categorization (n=664), MBF metrics did not provide additive discriminatory value when combined with perfusion quantitation (PQ AUC=0.795 [0.695-0.895], PQ + segmental SMBF AUC=0.801 [0.716-0.885], PQ + territory SMBF AUC=0.805 [0.721-0.888], PQ + segmental MFR AUC=0.784 [0.693-0.875], PQ + territory MFR AUC=0.783 [0.691-0.875], PQ + segmental RFR AUC=0.741 [0.613-0.870], PQ + territory RFR AUC=0.816 [0.730-0.902]).

Suppl. Figure 10A. Per-Vessel Diagnostic Performance of Perfusion Quantitation, Segmental, and Territory Flow Metrics for CAD 80-89% Categorization.

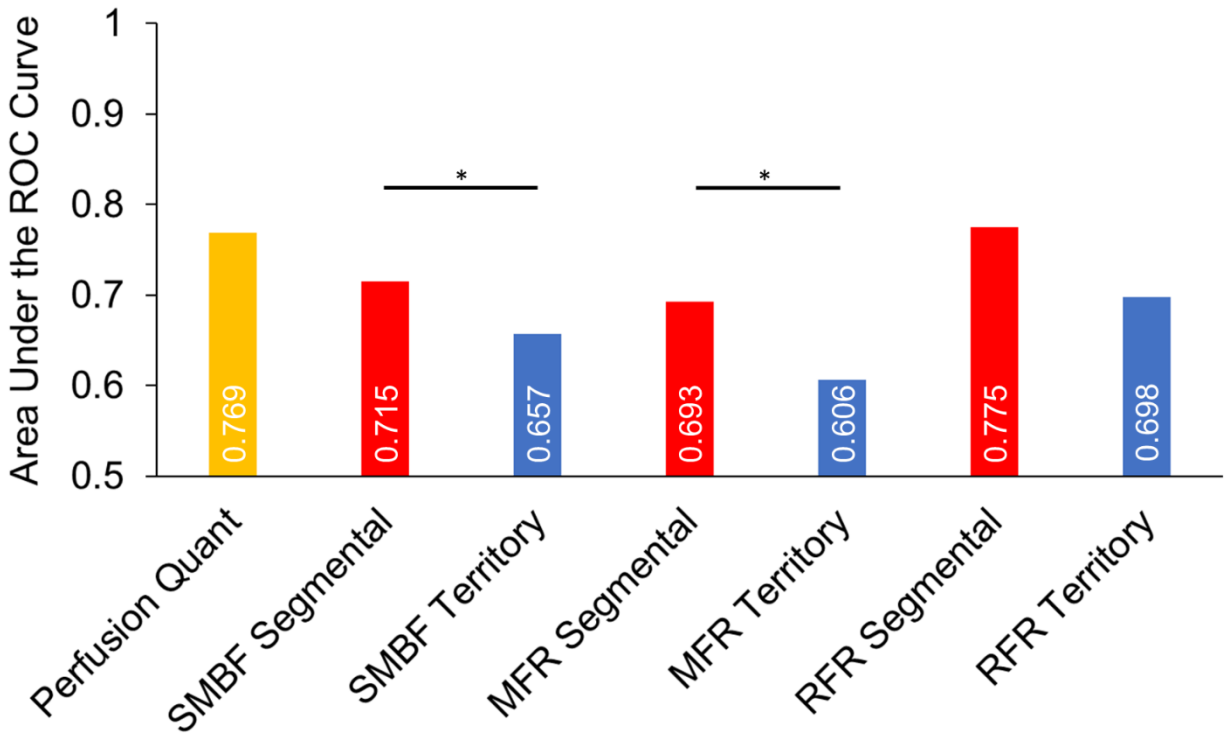

For CAD 80-89% categorization of pooled coronary territories (n=667), we conducted 3 sets of analyses. First, perfusion quantitation was compared with flow metrics. The perfusion quantitation AUC=0.769 (0.635-0.903) was similar to all segmental and territory flow metrics. Second, segmental and territory flow metrics were compared with each other. Segmental SMBF had a higher AUC=0.715 (0.595-0.834) than the territory SMBF AUC=0.657 (0.530-0.784). The segmental MFR AUC=0.693 (0.546-0.839) was also higher than the territory MFR AUC=0.606 (0.447-0.765). The segmental RFR AUC=0.775 (0.619-0.931) was not significantly different than the territory RFR AUC=0.698 (0.530-0.866). There was no significant difference when comparing the

diagnostic performances of SMBF, MFR, and RFR flow parameters with each other (*P<0.05).

Suppl. Figure 10B. Per-Vessel Diagnostic Performance of Combinatorial Perfusion Quantitation and Flow Metrics for CAD 80-89% Categorization.

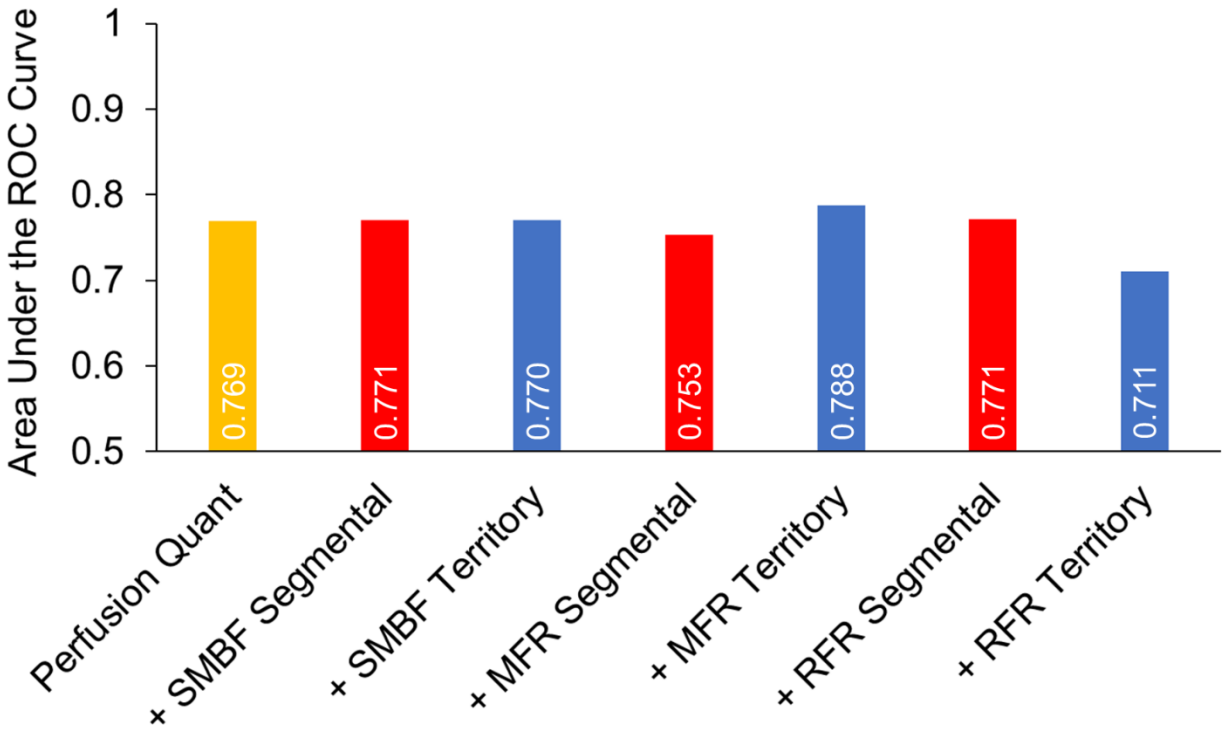

For CAD 80-89% categorization (n=667), MBF metrics did not provide additive discriminatory value when combined with perfusion quantitation (PQ AUC=0.769 [0.635-0.903], PQ + segmental SMBF AUC=0.771 [0.643-0.898], PQ + territory SMBF AUC=0.770 [0.646-0.895], PQ + segmental MFR AUC=0.753 [0.604-0.902], PQ + territory MFR AUC=0.788 [0.664-0.911], PQ + segmental RFR AUC=0.771 [0.613-0.929], PQ + territory RFR AUC=0.711 [0.534-0.887]).

Suppl. Figure 11A. Per-Vessel Diagnostic Performance of Perfusion Quantitation, Segmental, and Territory Flow Metrics for CAD 90-100% Categorization.

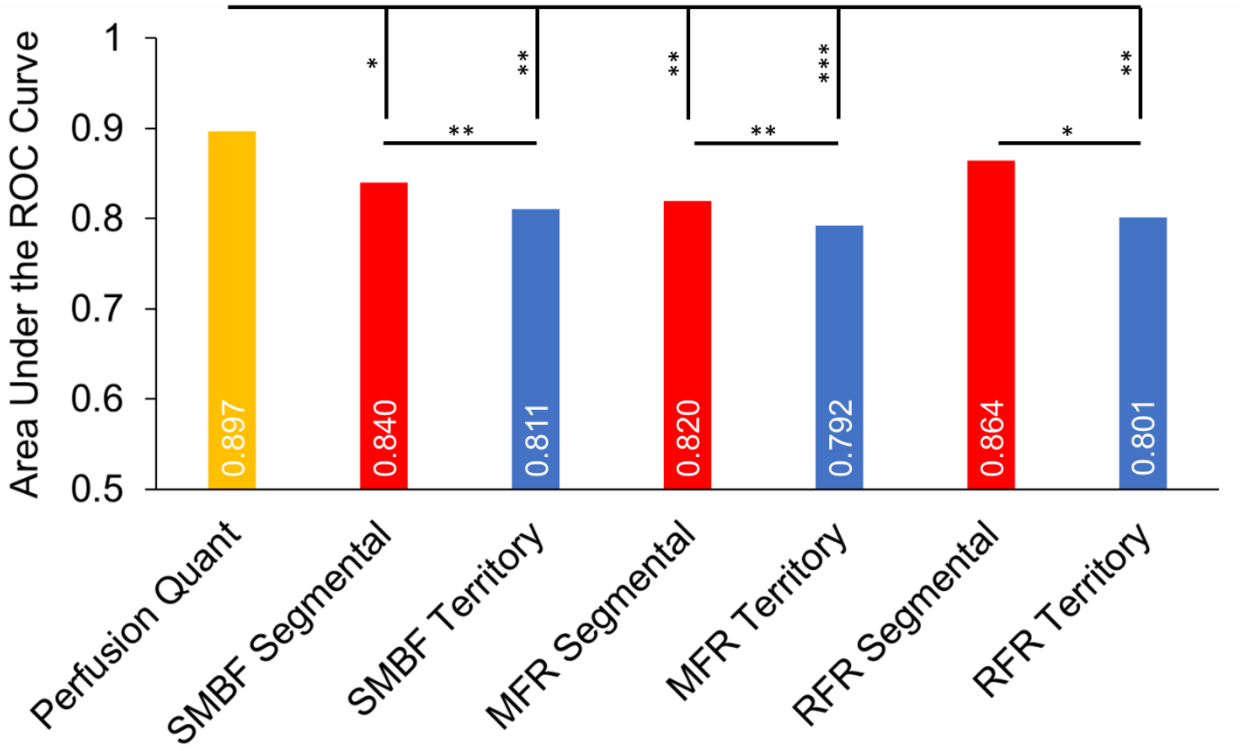

For CAD 90-100% categorization of pooled coronary territories (n=702), we conducted 3 sets of analyses. First, the perfusion quantitation AUC=0.897 (0.853-0.941) was significantly greater than all the flow metrics other than segmental RFR AUC=0.864 (0.800-0.928). Second, all the segmental flow metrics demonstrated significantly greater diagnostic performance than their territory counterparts (segmental SMBF AUC=0.840 [0.782-0.898] vs. territory SMBF AUC=0.811 [0.748-0.874]; segmental MFR AUC=0.820 [0.755-0.885] vs. territory MFR AUC=0.792 [0.726-0.859]; segmental RFR AUC=0.864 [0.800-0.928] vs. territory RFR AUC=0.801 [0.721-0.882]). The diagnostic performances of SMBF, MFR, and RFR flow parameters were not significantly different from each other (*P<0.05, **P<0.01, ***P<0.001).

Suppl. Figure 11B. Per-Vessel Diagnostic Performance of Combinatorial Perfusion Quantitation and Flow Metrics for CAD 90-100% Categorization.

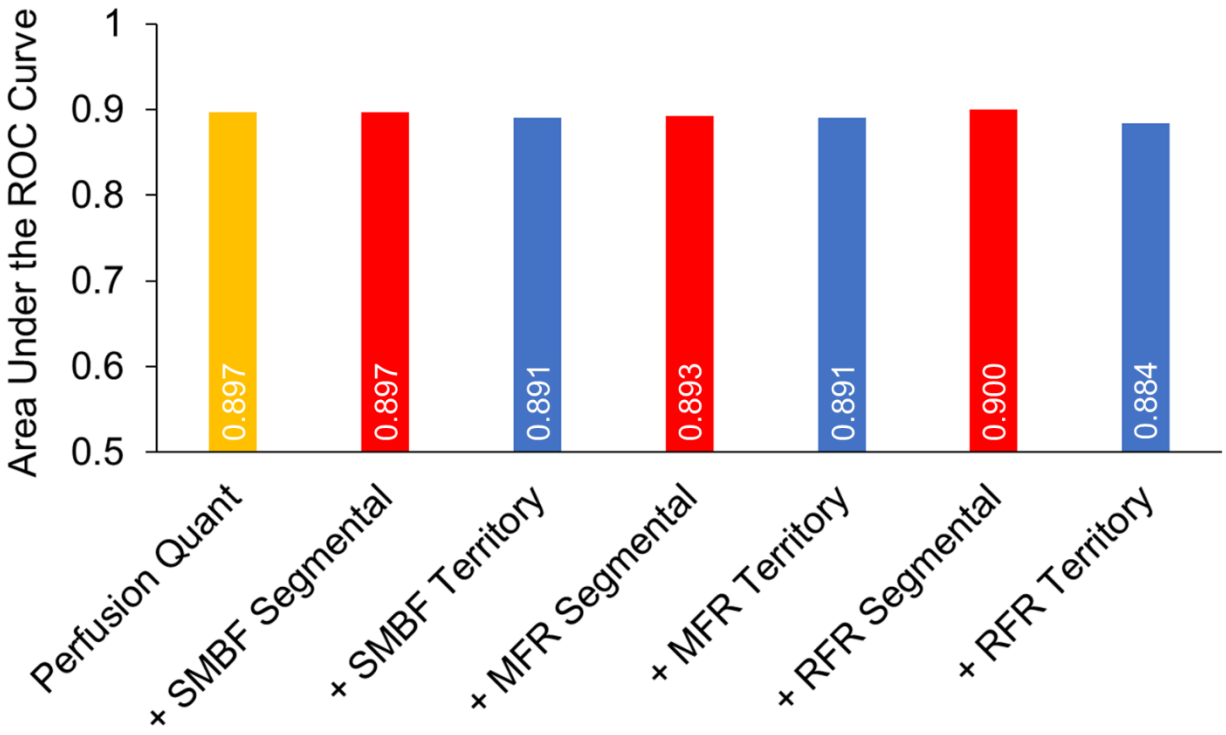

For CAD 90-100% categorization (n=702), MBF metrics did not provide additive discriminatory value when combined with perfusion quantitation (PQ AUC=0.897 [0.853-0.941], PQ + segmental SMBF AUC=0.897 [0.844-0.950], PQ + territory SMBF AUC=0.891 [0.835-0.946], PQ + segmental MFR AUC=0.893 [0.833-0.952], PQ + territory MFR AUC=0.891 [0.831-0.950], PQ + segmental RFR AUC=0.900 [0.854-0.947], PQ + territory RFR AUC=0.884 [0.828-0.940]).

Suppl. Figure 12. Per-Patient Diagnostic Performance of Segmental and Territory Flow Metrics for CAD ≥50% Categorization.

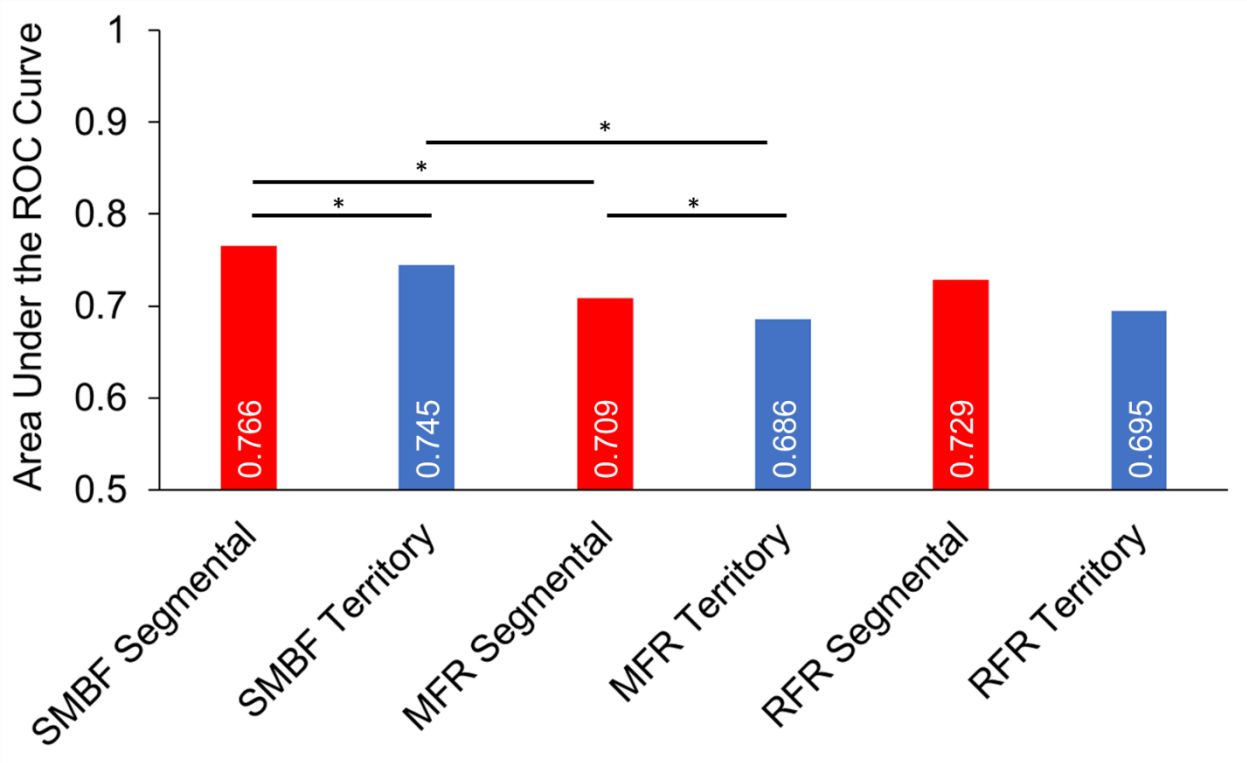

Bar graph depiction of Figure 5. In per-patient analyses (n=245), the segmental SMBF AUC=0.766 (0.706-0.825) was significantly greater than the territory SMBF AUC=0.745 (0.683-0.807) as well as the segmental MFR AUC=0.709 (0.642-0.777). The territory SMBF AUC=0.745 (0.683-0.807) was significantly greater than the territory MFR AUC=0.686 (0.617-0.756) (*P<0.05). The segmental RFR AUC=0.729 (0.663-0.796) was similar to the territory RFR AUC=0.695 (0.626-0.764).

Suppl. Figure 13. Per-Patient Diagnostic Performance of Segmental and Territory Flow Metrics for CAD ≥70% Categorization.

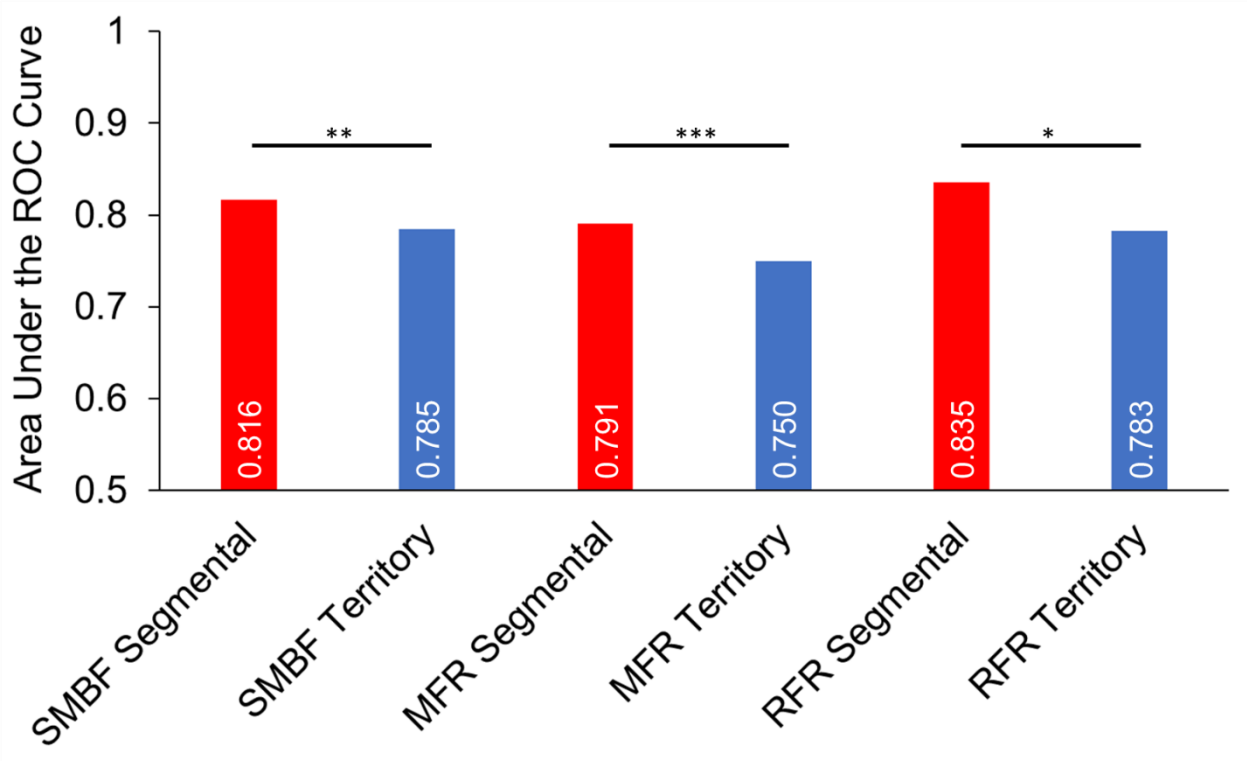

Bar graph depiction of Figure 6. In per-patient analyses (n=245), all the segmental flow metrics had a greater diagnostic performance than their territory counterparts, with segmental SMBF AUC=0.816 (0.755-0.877), territory SMBF AUC=0.785 (0.720-0.849), segmental MFR AUC=0.791 (0.727-0.855), territory MFR AUC=0.750 (0.680-0.820), segmental RFR AUC=0.835 (0.770-0.899), and territory RFR AUC=0.783 (0.709-0.856) (*P<0.05, **P<0.01, ***P<0.001).

Suppl. Figure 14. Case example of ^{18}F-flurpiridaz PET MPI in a 65 year-old male.

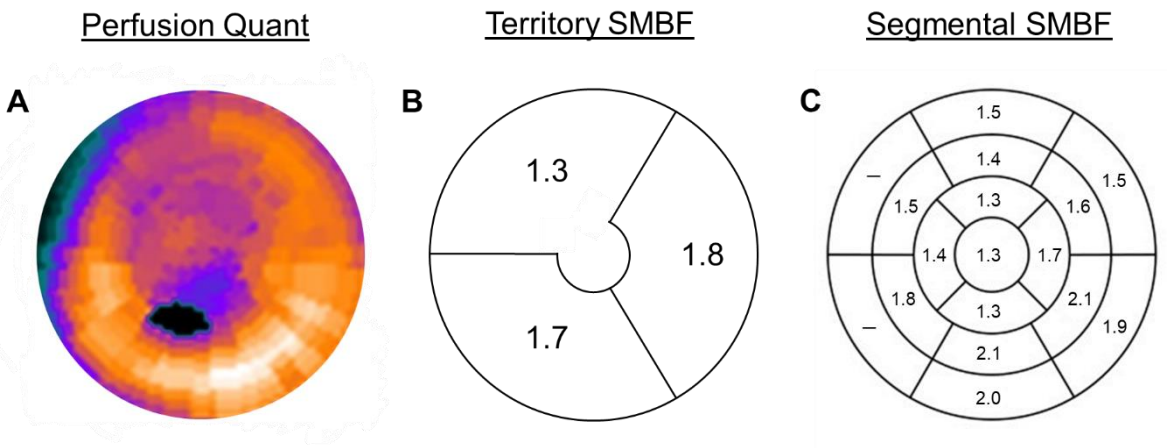

Automated relative perfusion quantitation did not detect significant CAD, with a deficit at stress of 2% globally (< to the previously validated threshold of ≥8% for CAD ≥50% stenosis detection[5]), and 0% in the LAD, LCx, and RCA territories. The territory SMBF was significant for a value of 1.3 $mL*min^{-1}*g^{-1}$ in the LAD territory, indicative of LAD disease. The segmental SMBF was significant for values of 1.3 $mL*min^{-1}*g^{-1}$ in the apical anterior segment and apex, indicative of LAD disease, and a value of 1.3 $mL*min^{-1}*g^{-1}$ in the apical inferior segment, indicative of RCA disease. Invasive coronary angiography demonstrated 64% LAD, 0% LCx, and 56% RCA stenoses. Thus, while relative perfusion quantitation was falsely normal, and territory SMBF only detected the LAD disease, segmental SMBF correctly identified 2-vessel CAD.

Suppl. Figure 15. Case example of ^{18}F-flurpiridaz PET MPI in a 52 year-old male.

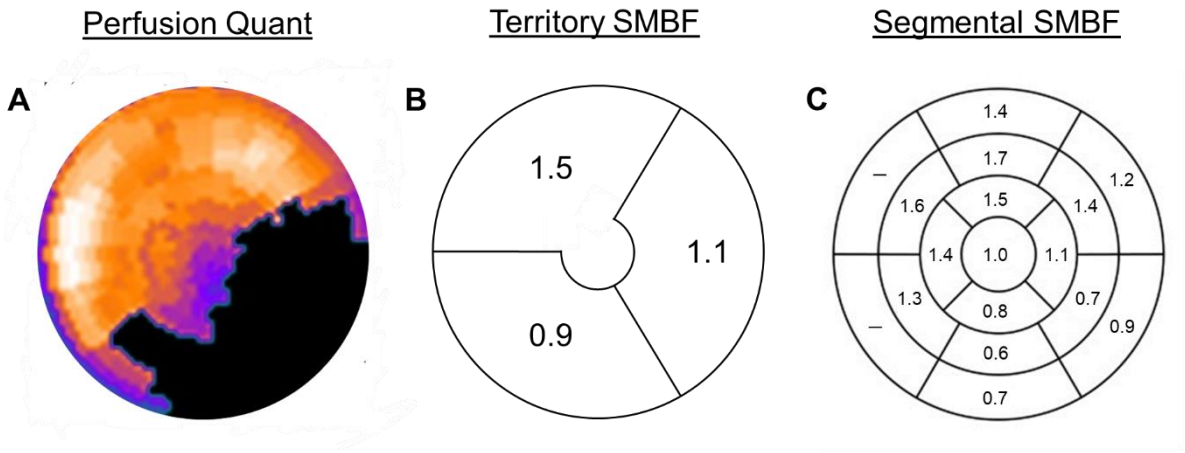

Automated relative perfusion quantitation demonstrated a deficit at stress of 34% globally, and 1% in the LAD, 93% in the LCx, and 66% in the RCA territories, consistent with significant CAD in the LCx and RCA territories. The territory SMBF was significant for a value of 1.1 $mL*min^{-1}*g^{-1}$ in the LCx territory, and 0.9 $mL*min^{-1}*g^{-1}$ in the RCA territory. The segmental SMBF was significant for values of 1.0 $mL*min^{-1}*g^{-1}$ in the apex, indicative of LAD disease, diffusely decreased values in the lateral segments with a lowest of 0.7 $mL*min^{-1}*g^{-1}$ in the mid inferolateral segment, indicative of LCx disease, and also diffusely decreased values in the inferior segments with a lowest of 0.6 $mL*min^{-1}*g^{-1}$ in the mid inferior segment, indicative of RCA disease. Invasive coronary angiography demonstrated 59% LAD, 66% LCx, and 100% RCA stenoses. Thus, while relative perfusion quantitation and territory SMBF both identified 2-vessel CAD, segmental SMBF correctly identified 3-vessel CAD.

Suppl. Table 1. Optimal Cutoff Points for CAD ≥50% and CAD ≥70% Stenosis

		Segmental			Territory		
		LAD	LCx	RCA	LAD	LCx	RCA
CAD ≥50%	SMBF	1.3	1.5	1.3	1.3	1.7	1.3
	MFR	2.2	2.1	2.3	2.5	2.4	2.7
	RFR	0.6	0.6	0.6	—	—	—
CAD ≥70%	SMBF	1.2	1.5	1.2	1.6	1.8	1.4
	MFR	2.1	2.3	1.9	2.6	2.6	2.3
	RFR	0.5	0.6	0.6	—	—	—

Detection.

Optimal cutoff points per coronary territory are presented for segmental and territory SMBF (in $mL*min^{-1}*g^{-1}$), segmental and territory MFR, and segmental RFR. **Legend.** SMBF: stress myocardial blood flow. MFR: myocardial flow reserve. RFR: relative flow reserve.